Supporting Information for:

Electrochemical Transformation of Trace Organic Contaminants in Latrine Wastewater

Justin T. Jasper, Oliver S. Shafaat, Michael R. Hoffmann

42 pages
13 figures
2 tables

Reaction Rate Constants for FAC and NH_2Cl. Test compound (100 nM) removal was followed in buffered solutions (pH 8.7; 20 mM borate) with excess FAC (0.03-5.0 mM) or NH_2Cl (0.3-3.0 mM). NH_2Cl solutions were prepared by adding stock solutions of FAC dropwise to excess NH_4Cl (1.2:1 NH_4Cl:HOCl). Samples were quenched (45 mM Na_2S_2O3) prior to analysis. Solution pH values and total chlorine concentrations did not change significantly over the course of the experiments. Rate constants were calculated based on first-order removal kinetics of the test compounds using measured steady-state total chlorine concentrations. For ciprofloxacin, rate constants were measured at multiple NH_2Cl and FAC concentrations to verify that observed ciprofloxacin transformation rates were not dependent on oxidant concentrations, but rather represented decay of the rapidly formed N-chlorinated ciprofloxacin intermediate as previously reported.[1] First-order ciprofloxacin decay rates were therefore reported.

Reaction Rate Constants for the Chlorine Radical Anion, $\cdot Cl_2^-$. Second-order rate constants for the reaction of test compounds with the dichlorine radical anion ($\cdot Cl_2^-$) were measured by nanosecond transient absorption laser flash photolysis of solutions containing $Na_2S_2O_8$ (25 mM), NaCl (100 mM), and test compounds (0-100 μM). Excitation at 266 nm (8 ns FWHM, 10 Hz repetition rate) produced $\cdot SO_4^-$ that rapidly reacted with Cl^- to produce $\cdot Cl_2^-$ (~1 μM). Solution pH values ranged from 5.5 to 6.0. The decay of $\cdot Cl_2^-$ was monitored at 340 nm over 10 ms, and data was averaged over 10 shots. $\cdot Cl_2^-$ decay was log-normalized and plotted versus test compound concentrations to determine second-order rate constants. $\cdot Cl_2^-$ decay was log-normalized and fit according to:

$$A(340) = fe^{-gt} + h \quad \text{(S1)}$$

where A(340) is the absorbance at 340 nm, f is the initial absorbance, g is the decay rate, and h is an offset due to a longer lived species formed after $\cdot Cl_2^-$ decay.[2] $\cdot Cl_2^-$ decay rates were plotted versus test compound concentrations to determine second-order rate constants:

$$g = k_{cmpd,\cdot Cl_2^-}[cmpd] + b \quad \text{(S2)}$$

where $k_{cmpd,\cdot Cl_2^-}$ is the second-order rate constant for the reaction of a test compound with $\cdot Cl_2^-$, [cmpd] is the test compound concentration, and b is the y-intercept that represents loss of $\cdot Cl_2^-$ due to other reactions (e.g., quenching by H_2O). Under these conditions ·Cl is predicted to contribute less than 5% to measured second-order rate constants greater than 10^7 M^{-1} s^{-1}.

Chronoamperometric Experiments. Chronoamperometric experiments were performed to verify direct electron transfer for compounds that underwent transformation in the absence of Cl^- and were soluble enough dissolve rapidly (i.e., ranitidine and cimetidine). About 5 mM of a solid test compound was added to a solution of Na_2SO_4 (20 mM) undergoing potentiostatic electrolysis (3.5 V cathode vs. anode), and the current response was observed. A spike in the current upon test compound addition implied that the compound could be oxidized directly at the anode.[3,4] The possibility that current increased due to a change in electrolyte strength was eliminated based on the current's return to near baseline values after test compound oxidation was complete.

Transformation Product Identification. Test compound transformation product formulae were calculated based on accurate masses and typically had a mass error of less than 2 mDa (Table SI 2). Transformation product halogen content was confirmed by characteristic isotopic patterns using the m/z+2, m/z+4, etc. peaks. Isotopic peak ratios were typically within 10% of theoretical values for the proposed formulae. Transformation product structures were proposed based on the literature when possible (see bold references in Table SI 2), by comparing exact mass values and fragment ions. In other cases, structures were proposed simply based on determined formulae. In these cases, the exact position of certain functional groups (e.g., hydroxyl and chlorine) could not be determined. When possible, proposed structures were verified with authentic standards, as specified in Table SI 2.

Analytical Methods. Dissolved organic carbon and dissolved inorganic carbon were measured by persulfate digestion using an Aurora TOC analyzer.[5] NO_3^-, Cl^-, PO_4^{3-}, SO_4^{2-}, and NH_4^+ were analyzed by ion chromatography (Dionex ICS 2000; AS19G anions, CS12A cations).[5]

Test compounds were separated by an Acquity BEH C18 column (2.1x50 mm; 1.7 μm particles), eluted at 0.5 mL min^{-1} using acetonitrile and water with 0.1% formic acid and 1% acetonitrile. The following gradient was used: 0 min, 5% acetonitrile; 0.2 min, 5% acetonitrile; 3.2 min, 95% acetonitrile; 3.5 min, 95% acetonitrile; 3.6 min, 5% acetonitrile; 5 min, 5% acetonitrile. Column temperature was held at 35 °C. pCBA were detected by UV absorbance (270 nm). Trace organic compounds were detected by positive electrospray ionization (ESI+) in resolution mode with a capillary voltage of 0.2 kV, a cone voltage of 50 V, and a source offset of 80 V. Source temperature was 120 °C and desolvation temperature was 400 °C. Cone gas was 40 L/h and desolvation gas was 800 L/h. Scan time was 0.3 s in continuum mode. A collision energy of 1.0 eV was used. A second acquisition channel scanned collision energy from 0-30 eV for fragment identification. Accurate mass values were corrected by the software using a leucine lock-mass.

Calculation of $\cdot Cl_2^-$ Reaction with Propranolol. The fraction of $\cdot Cl_2^-$ reacting with propranolol ($F_{\cdot Cl_2^-,propranolol}$) in latrine wastewater (100 mg L^{-1} TOC) was calculated using $\cdot Cl_2^-$ measured second-order reaction rate constants with propranolol ($k_{\cdot Cl_2^-,propranolol}$) and TOC ($k_{\cdot Cl_2^-,TOC}$) to be:

$$F_{\cdot Cl_2^-,propranolol} = \frac{k_{\cdot Cl_2^-,propranolol}[propranolol]}{k_{\cdot Cl_2^-,propranolol}[propranolol] + k_{\cdot Cl_2^-,TOC}[TOC]}$$

$$= \frac{1.9x10^9\ M^{-1}\ s^{-1} * \ 1x10^{-6}\ M}{1.9x10^9\ M^{-1}\ s^{-1} * \ 1x10^{-6}\ M + 1.9x10^3\ (mg\ L^{-1})^{-1}\ s^{-1} * \ 100\ mg\ L^{-1}}$$

$$= 0.0099$$

Test Compound Transformation Products. Carbamazepine's predominant transformation products were confirmed to be acridine, hydroxyacridine, and acridine-9-carboxaldehyde (Table SI 2; Figures SI 12a and 13), based on authentic standards. No chlorinated transformation products were identified during latrine wastewater or buffered Cl^- solution electrolysis. Transformation products were similar to those previously observed during oxidation and chlorination of carbamazepine.[6–10]

Metoprolol and propranolol were predominantly transformed to chlorinated products that underwent further transformation to form products not detected by LCMS (Figures SI 12b,c and 9). Hydroxylated and multiply halogenated transformation products were also identified (Table SI 2). Most metoprolol transformation products were identified previously during reverse osmosis retentate electrolysis[11] or other treatment processes.[12,13] Some propranolol transformation products observed in this study have been reported previously,[14–17] but others have not, including the predominant chlorinated product (m/z 294.1276 amu; m/z+2 amu observed at ~33%).

Identified ciprofloxacin transformation products were typically transformed at the piperazine group rather than chlorinated (Figures SI 12d, 13), as previously observed during ciprofloxacin reaction with FAC and ClO_2.[1,18]

Trimethoprim was transformed into a variety of hydroxylated and chlorinated transformation products, some of which have been identified during treatment using ferrate,[19] activated sludge,[20] and FAC.[21]

Only a few significant acetaminophen and cimetidine transformation products were observed (Figures SI 12f and 13), all of which are produced by reaction with FAC.[22–24] As with

trimethoprim, different acetaminophen transformation products were observed in the absence of NH_4^+, including formation of dichlorinated acetaminophen.

Ranitidine transformation products were chlorinated, demethylated, and oxidized, with the latter two transformations likely occurring at the furan group.[25] Although a few of the identified products have previously been observed during chloramination of ranitidine,[25] further work is needed to confirm transformation product structures (Table SI 2). Many transformation products observed during latrine wastewater electrolysis were not observed during electrolysis of buffered Cl^- solutions (Figures SI 12g and 13; see main text).

Table SI 1. Comparison of Measured Test Compound Reaction rates with HOCl and NH_2Cl to Literature Values.

compound	property					
	k_{FAC} ($M^{-1}s^{-1}$) [a,b]		k_{NH_2Cl} ($M^{-1}s^{-1}$) [a]		k_{Cl_2} ($M^{-1}s^{-1}$)	
	measured	literature	measured	literature	measured	literature
carbamazepine	$8.9(\pm1.0)\times10^{-2}$	2.7×10^{-2} (10)	$<3\times10^{-3}$	n.a. [c]	$\sim1\times10^{5}$	6.7×10^{4} (16)
metoprolol	$1.9(\pm1.0)\times10^{-2}$	2×10^{-2} (16)	$<4\times10^{-3}$	<0.1 (16)	$\sim4\times10^{3}$	$0.6\text{-}1.4\times10^{3}$ (16,26) [d]
propranolol	$0.27(\pm0.02)$	0.3 (16)	$<6\times10^{-3}$	<0.1 (16)	$\sim2\times10^{5}$	3.3×10^{5} (16) [d]
ciprofloxacin	$5.6(\pm0.4)\times10^{-4}$ s^{-1} [e]	7×10^{-4} s^{-1} (1) [e]	9×10^{-4} s^{-1} [e]	7×10^{-4} s^{-1} (1) [e]	$\sim6\times10^{3}$	4.3×10^{3} (1) [f]
trimethoprim	$6.7(\pm0.2)$	8 (21)	$<1\times10^{-3}$	negligible (21)	$\sim3\times10^{6}$	$2\times10^{5}\text{-}2\times10^{6}$ (21)
acetaminophen	$7.0(\pm0.4)\times10^{2}$	$0.7\text{-}1.4\times10^{2}$ (16,23,27)	$0.9(\pm0.1)$	1.1×10^{-2} (16)	$\sim3\times10^{4}$	n.a. [c]
ranitidine	$>8\times10^{3}$	n.a. [c]	11(±1)	12 (25)	$\sim8\times10^{4}$	n.a. [c]
cimetidine	$>6.5\times10^{3}$	$>1\times10^{3}$ (24) [g]	47(±1)	48 (24)	$\sim4\times10^{6}$	n.a. [c]

[a] Measured or calculated at pH 8.7. [b] FAC=[HOCl]+[OCl^-]. [c] n.a.: not available. [d] Calculated at pH 1.3 based on reported acid catalyzed reactions with HOCl. [e] First-order transformation rate is reported due to rapid quenching of the N-chlorinated ciprofloxacin intermediate by $Na_2S_2O_3$. [f] Reaction rate between HOCl and the predominant fully protonated form of ciprofloxacin at pH 1.3. [g] Estimated based on complete removal within 10 s.

153 Table SI 2. Test Compound Transformation Products (TPs).

Parent Test compound	TP m/z [a] (ID)	Major Fragment ions m/z	RT (min)	Calculated Formula	Mass Error (mDa)	Proposed Molecular Ion Structure [b]	Refs.[c]
Carbamazepine	224.0715 (Cbz 224)	164.920, 167.073, 180.081, 196.076	0.58	$C_{14}H_{10}NO_2$	0.3	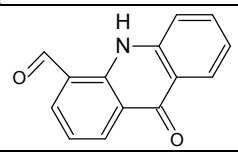	6,7
	180.0812 [d] (Cbz 180)	152.0621	1.17	$C_{13}H_{10}N$	0.3	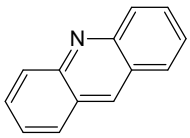	6,8
	275.0800 (Cbz 275)	180.0800, 210.0919, 236.0712, 253.0976	1.58	$C_{14}H_{13}NO_5$	0.6		
	253.0974 [d] (Cbz 253)		1.59	$C_{15}H_{13}N_2O_2$	0.3	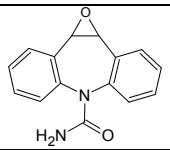	6,10
	196.0759 [e] (Cbz 196)	167.073, 180.0810	1.65	$C_{13}H_{10}NO$	0.3	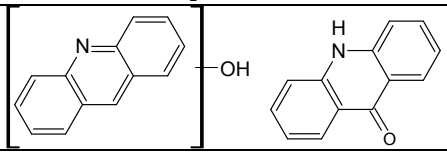	6–9
	208.0761 [d] (Cbz 208)	152.062, 180.082, 196.0760	2.07	$C_{14}H_{10}NO$	0.1	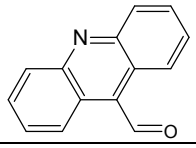	8,9
Metoprolol	226.1436 (Met 226)	116.1067, 121.0636, 149.0583	0.82	$C_{12}H_{20}NO_3$	0.7	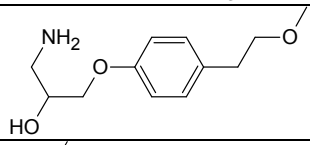	11,13
	284.1853 (Met 284)	116.1063, 226.1420, 268.141	0.85	$C_{15}H_{26}NO_4$	0.9	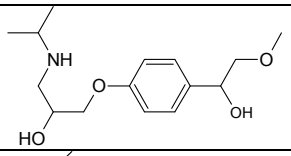	11,13
	254.1393 (Met 254)	105.0692, 151.0381, 177.0540, 212.0911, 236.1275	0.93	$C_{13}H_{20}NO_4$	<0.1	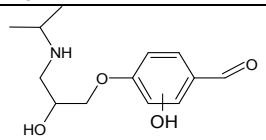	
	238.1439 (Met 238)	105.0696, 133.0642, 149.0590 161.0589, 196.0962	1.04	$C_{13}H_{20}NO_3$	0.4	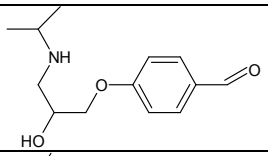	12
	282.1706 (Met 282)	105.0696, 133.0642, 149.0590 161.0589, 196.0962	1.05	$C_{15}H_{24}NO_4$	<0.1	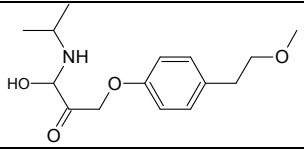	11

Parent Test compound	TP m/z [a] (ID)	Major Fragment ions m/z	RT (min)	Calculated Formula	Mass Error (mDa)	Proposed Molecular Ion Structure [b]	Refs.[c]
Metoprolol (cont.)	**302.1515** (Met 302)	98.0963, 116.1066, 167.0249, 193.0407, 260.1044, 284.1411	1.51	$C_{15}H_{25}NO_3Cl$	0.8	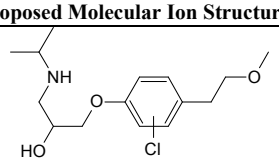	11
	336.1121 (Met 336)	72.0817, 98.0965, 116.1064, 276.0549, 294.0649, 318.102	1.62	$C_{15}H_{24}NO_3Cl_2$	1.2	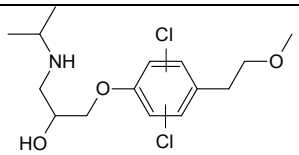	11
Propranolol	276.1599 (Pro 276)	116.1074	1.0-1.3 [f]	$C_{16}H_{22}NO_3$	<0.1	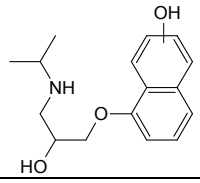	17
	292.1545 (Pro 292)	116.107, 123.092, 150.128, 274.144, 272.128,	1.29	$C_{16}H_{22}NO_4$	0.4	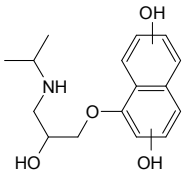	15
	218.1180 (Pro 218)	116.1071, 183.0804	1.45	$C_{13}H_{16}NO_2$	0.1	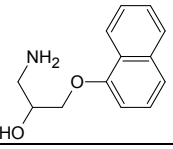	16
	310.1210 (Pro 310)	72.0816, 116.1071, 135.1038, 260.1653	1.53	$C_{16}H_{21}NO_3Cl$	<0.1	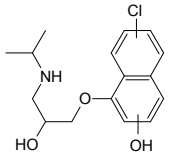	
	294.1276 (Pro 294)	150.128, 260.165	1.85	$C_{16}H_{21}NO_2Cl$	1.5	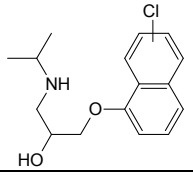	
	338.0739 (Pro 338)	116.1070, 182.0725, 217.0417	1.94	$C_{16}H_{21}NO_2Br$	1.7	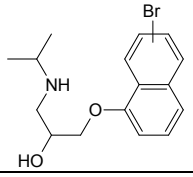	
	328.0868 (Pro 328)	72.0819, 116.1068, 219.1751	1.98	$C_{16}H_{20}NO_2Cl_2$	0.3	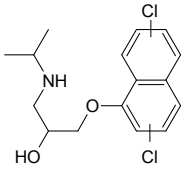	

Parent Test compound	TP m/z [a] (ID)	Major Fragment ions m/z	RT (min)	Calculated Formula	Mass Error (mDa)	Proposed Molecular Ion Structure [b]	Refs.[c]
Ciprofloxacin	306.1246 (Cfx 306)	217.0404, 268.1077, 288.1142	1.09	$C_{15}H_{17}N_3O_3F$	0.8	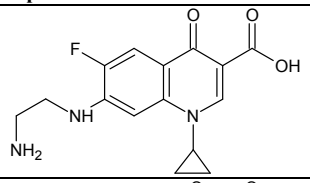	1,18
	366.1012 (Cfx 366)	225.0213, 245.1079, 279.0695, 322.1108	1.22	$C_{17}H_{18}N_3O_3FCl$	0.9	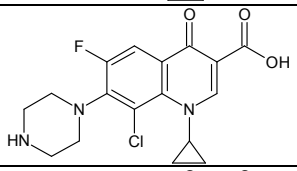	1
	362.1141 (Cfx 362)	344.1037	1.29	$C_{17}H_{17}N_3O_5F$	1.1	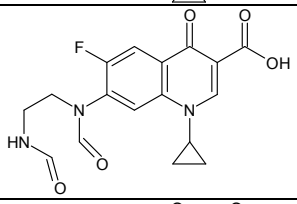	18
	291.0773 (Cfx 291)	245.0709, 273.0671	1.42	$C_{14}H_{12}N_2O_4F$	0.8	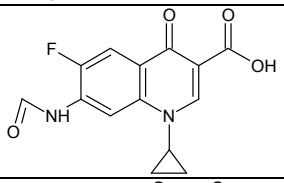	
	263.0828 (Cfx 263)	204.032, 245.0724	1.49	$C_{13}H_{12}N_2O_3F$	0.4	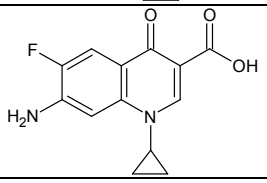	18
	298.0287 (Cfx 298)	280.0184	1.63	$C_{13}H_{10}NO_4FCl$	0.5		1
	289.0981 (Cfx 289)	271.0876	1.74	$C_{15}H_{14}N_2O_3F$	0.8	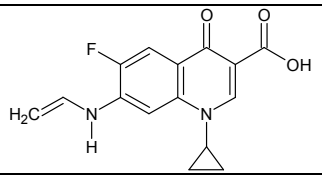	
Trimethoprim	**342.1327** (Tmp 342)	273.0978, 307.1397	0.98	$C_{14}H_{21}N_5O_3Cl$	0.6		
	307.1391 (Tmp 307)	209.1644, 212.0686, 240.0634, 258.0742, 273.0975	0.98	$C_{14}H_{19}N_4O_4$	1.5	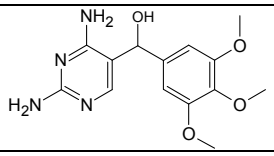	19
	322.1508 (Tmp 322)		1.04	$C_{14}H_{20}N_5O_4$	0.7		
	325.1499 (Tmp 325a)	173.0813, 219.0872, 233.1043, 293.1229	1.05	$C_{14}H_{21}N_4O_5$	1.3	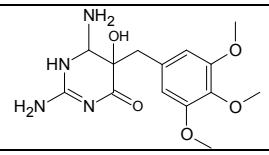	20
Trimethoprim	**343.1164** (Tmp 343)	181.0852	1.08	$C_{14}H_{20}N_4O_4Cl$	0.9	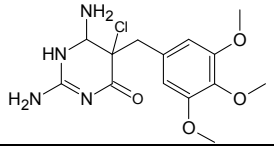	

Parent Test compound	TP m/z [a] (ID)	Major Fragment ions m/z	RT (min)	Calculated Formula	Mass Error (mDa)	Proposed Molecular Ion Structure [b]	Refs.[c]
(cont.)	**359.1125** (Tmp 359a)	215.0465, 240.0414, 236.0905	1.19	$C_{14}H_{20}N_4O_5Cl$	0.3	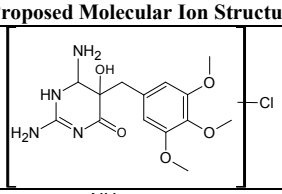	
	323.1345 (Tmp 323)		1.26	$C_{14}H_{19}N_4O_5$	1.0	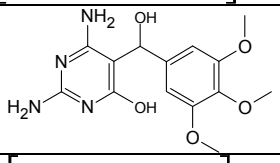	
	377.0773 (Tmp 377)	217.0435, 236.0913, 255.0416, 257.0388, 314.0898	1.26	$C_{14}H_{19}N_4O_4Cl_2$	1.0	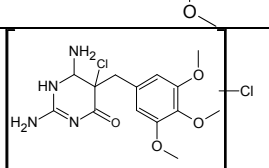	21
	393.0719 (Tmp 393)	100.0503, 126.0529, 249.0075, 270.0524	1.32	$C_{14}H_{19}N_4O_5Cl_2$	1.4	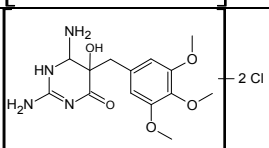	
	325.1059 (Tmp 325b)	145.0267, 271.0918, 249.008	1.39	$C_{14}H_{18}N_4O_3Cl$	0.8	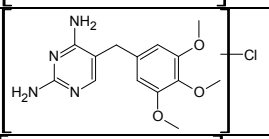	21
	411.0391 (Tmp 411)	249.0080, 366.0616	1.39	$C_{14}H_{18}N_4O_4Cl_3$	0.3	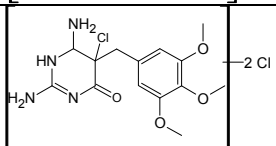	21
	369.0558 (Tmp 369)	255.0886, 273.092, 325.1078, 339.0081	1.42	$C_{14}H_{18}N_4O_3Br$	0.4	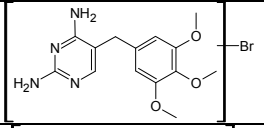	
	359.0672 (Tmp 359b)	181.0854, 199.097, 289.0480, 298.0371, 329.0196	1.55	$C_{14}H_{17}N_4O_3Cl_2$	0.6	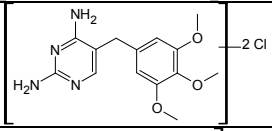	21
	403.0174 (Tmp 403)	140.0686, 180.8981, 257.1478, 359.0669	1.58	$C_{14}H_{17}N_4O_3BrCl$	0.1	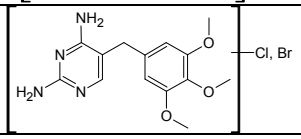	
Acetaminophen	**186.0312** (Ace 186)	109.0515, 144.0201, 155.9838	1.17	$C_8H_9NO_2Cl$	1.0	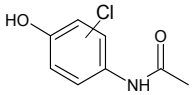	22,23
	219.9919 (Ace 219)	143.0123, 177.9810	1.42	$C_8H_8NO_2Cl_2$	1.3	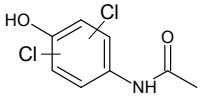	22,23
Ranitidine	**338.0561** (Rnt 338)	109.0278, 186.0565, 202.9997, 214.0240, 292.0612	0.63	$C_{11}H_{17}N_3O_5SCl$	1.6	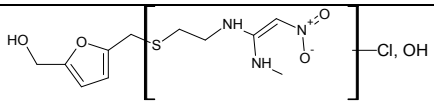	25

Parent Test compound	TP m/z [a] (ID)	Major Fragment ions m/z	RT (min)	Calculated Formula	Mass Error (mDa)	Proposed Molecular Ion Structure [b]	Refs.[c]
	336.0419 (Rnt 336)	125.0600, 181.0201, 203.0023, 214.0259, 290.0497	0.66	$C_{11}H_{15}N_3O_5SCl$	0.2	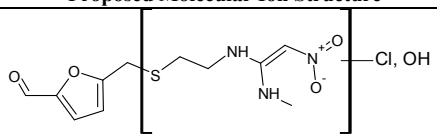	
	364.1194 (Rnt 364)	109.0278, 163.0854, 189.1012, 258.0579	0.76	$C_{13}H_{23}N_5O_3SCl$	1.6	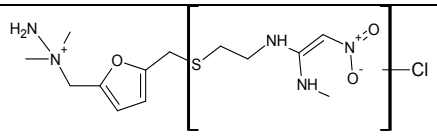	25
	335.0928 (Rnt 335)		0.85	$C_{12}H_{20}N_4O_3SCl$	1.6	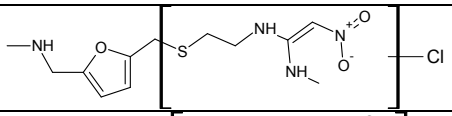	
	349.1083 (Rnt 349)	124.075, 132.0438, 164.0159, 210.0092, 223.0893	0.88	$C_{13}H_{22}N_4O_3SCl$	1.8	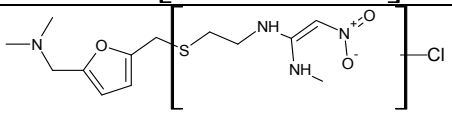	25
	270.0903 (Rnt 270)	97.0759, 165.1013, 191.1167, 224.0971	1.02	$C_{11}H_{16}N_3O_3S$	0.9		
	322.061 (Rnt 322)	165.0236, 240.1152	1.08	$C_{11}H_{17}N_3O_4SCl$	1.8	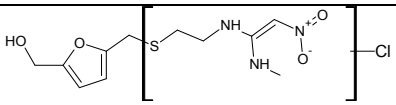	
	320.0459 (Rnt 320)	109.028, 165.0238, 208.0392, 234.0191, 274.0529	1.12	$C_{11}H_{15}N_3O_4SCl$	1.3	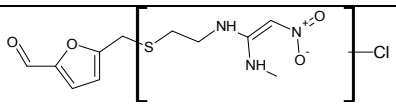	
	294.12575 (Rnt 294)	109.0294, 150.1284, 177.0489, 188.0054, 275.053	1.85	$C_{13}H_{25}NO_2SCl$	3.7		
Cimetidine	**117.0210** (Cmt 117)	90.0104	0.53	$C_4H_6N_2Cl$	1.0	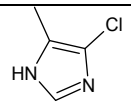	24
	189.0435 (Cmt 189)	82.0403	1.06	$C_5H_9N_4O_2S$	1.1	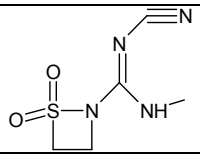	24

[a] Compounds with m/z ratios in bold exhibited isotopic patterns consistent with the halogen atoms specified in the calculated formula (i.e., m/z+2, m/z+4, etc. peaks). [b] Structure of unprotonated TP. Structure based on calculated formula, fragments, and literature. [c] References in bold proposed compound structure shown. References in italics observed similar major fragment ions. [d] TP identity confirmed based on authentic standard retention time and mass spectrum. [e] Authentic acridone standard (ketone product shown) retention time differed by ~0.03 min and had different fragmentation pattern, suggesting that hydroxyacridone was formed during electrolysis. [f] Multiple peaks observed.

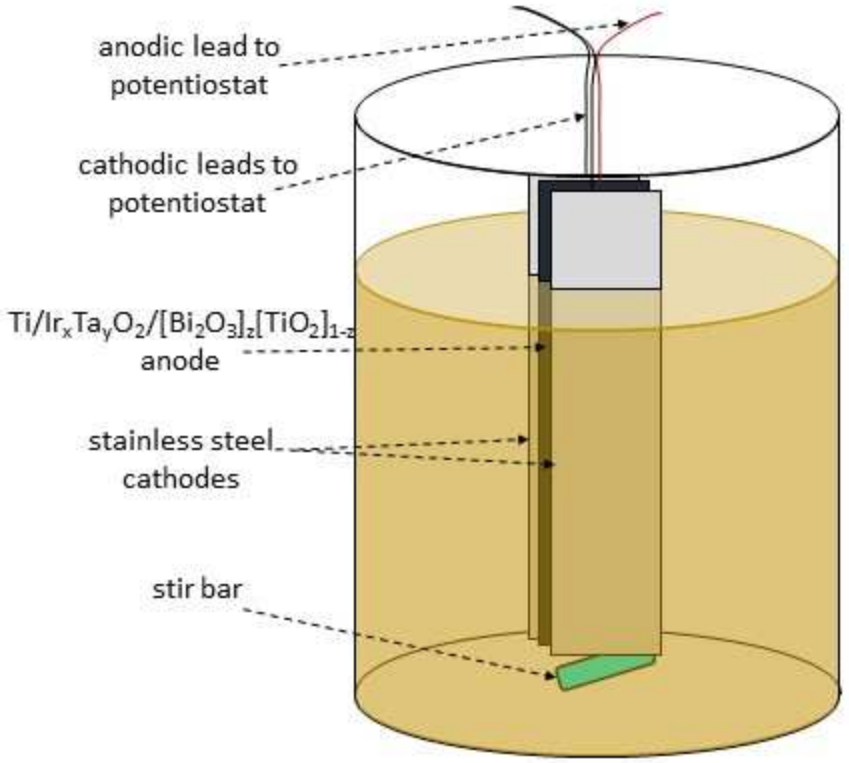

Figure SI 1. Schematic of electrochemical reactor used in this study.

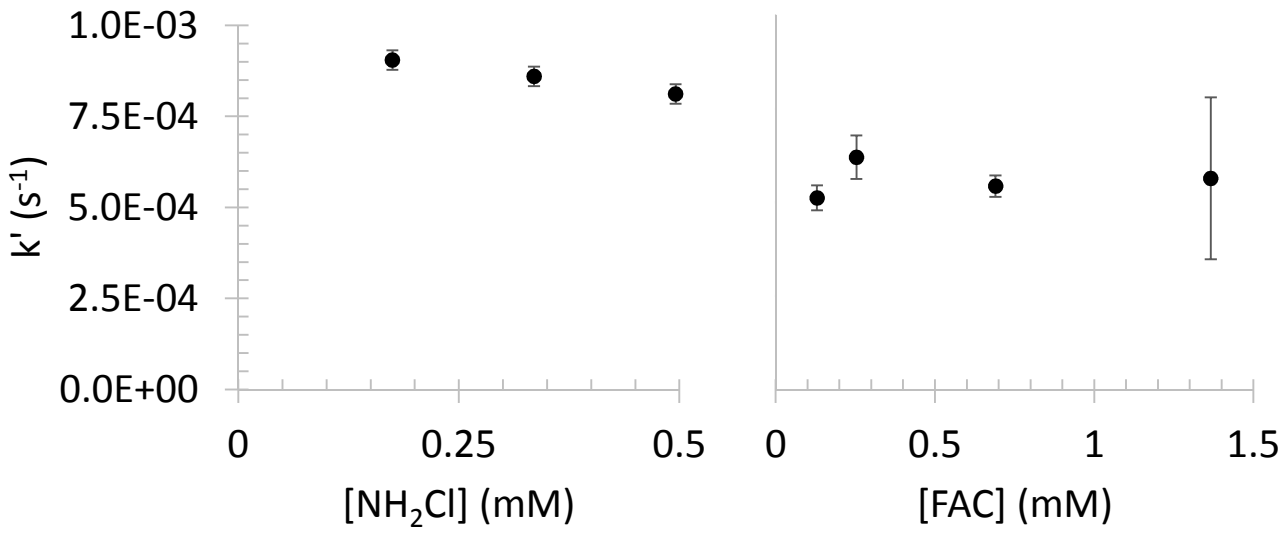

Figure SI 2. Measured first-order rate constants for the reaction of ciprofloxacin with various concentrations of NH_2Cl and FAC. Error bars represent ± one standard deviation.

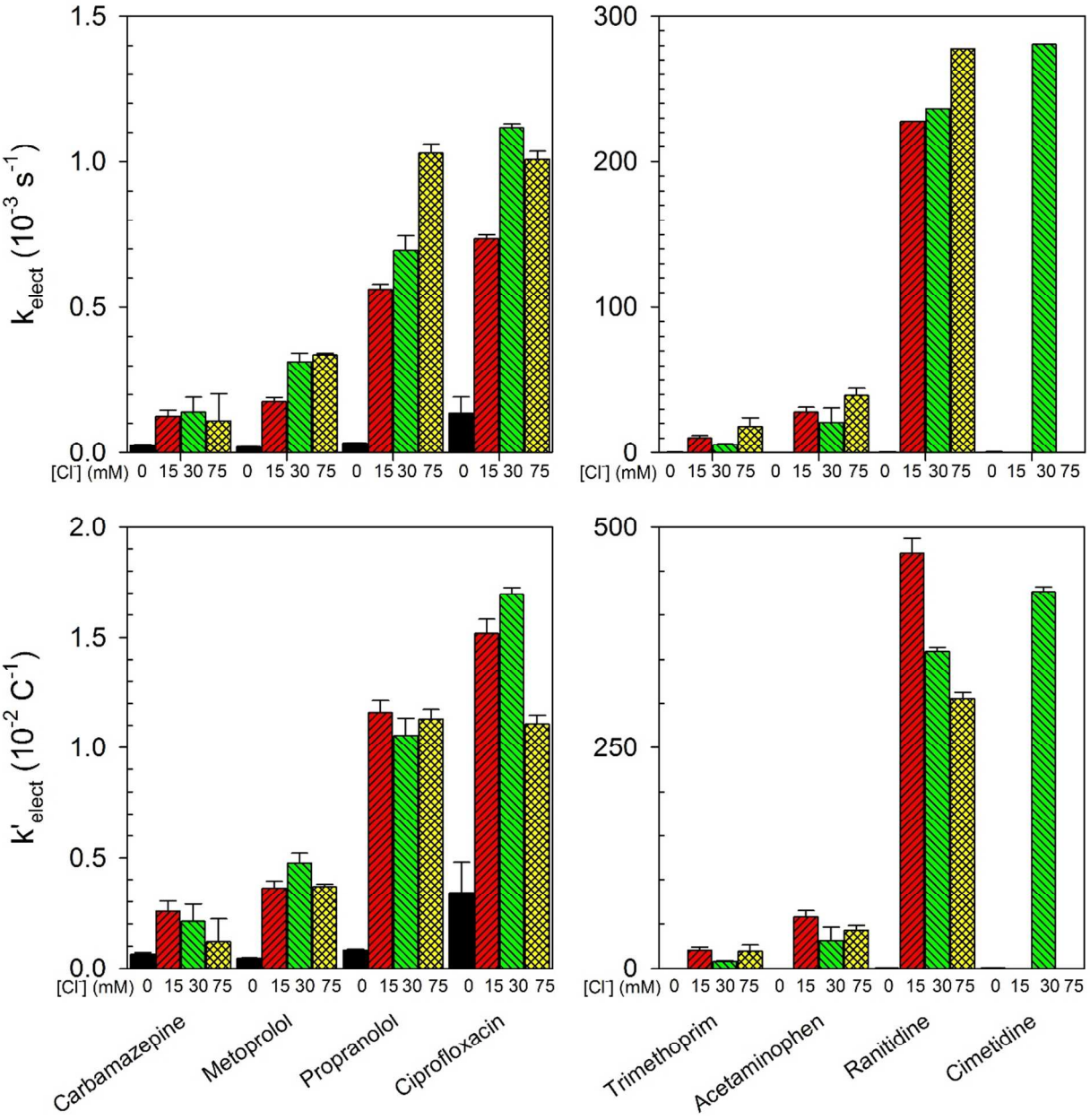

Figure SI 3. Pseudo-first order test compound electrolysis rates (k; top) and rates normalized for charge (k′; bottom). Solutions were electrolyzed at an applied potential of 3.5 V in 0-75 mM NaCl solution buffered at pH 8.7 (20 mM borate). Average current densities: 0 mM, 0.6 A L^{-1}; 15 mM, 0.7 A L^{-1}; 30 mM, 0.9 A L^{-1}; 75 mM, 1.3 A L^{-1}. FAC production rates: 15 mM, 0.9 μM s^{-1}; 30 mM, 1.6 μM s^{-1}; 75 mM, 3 μM s^{-1}. Error bars represent ± one standard deviation.

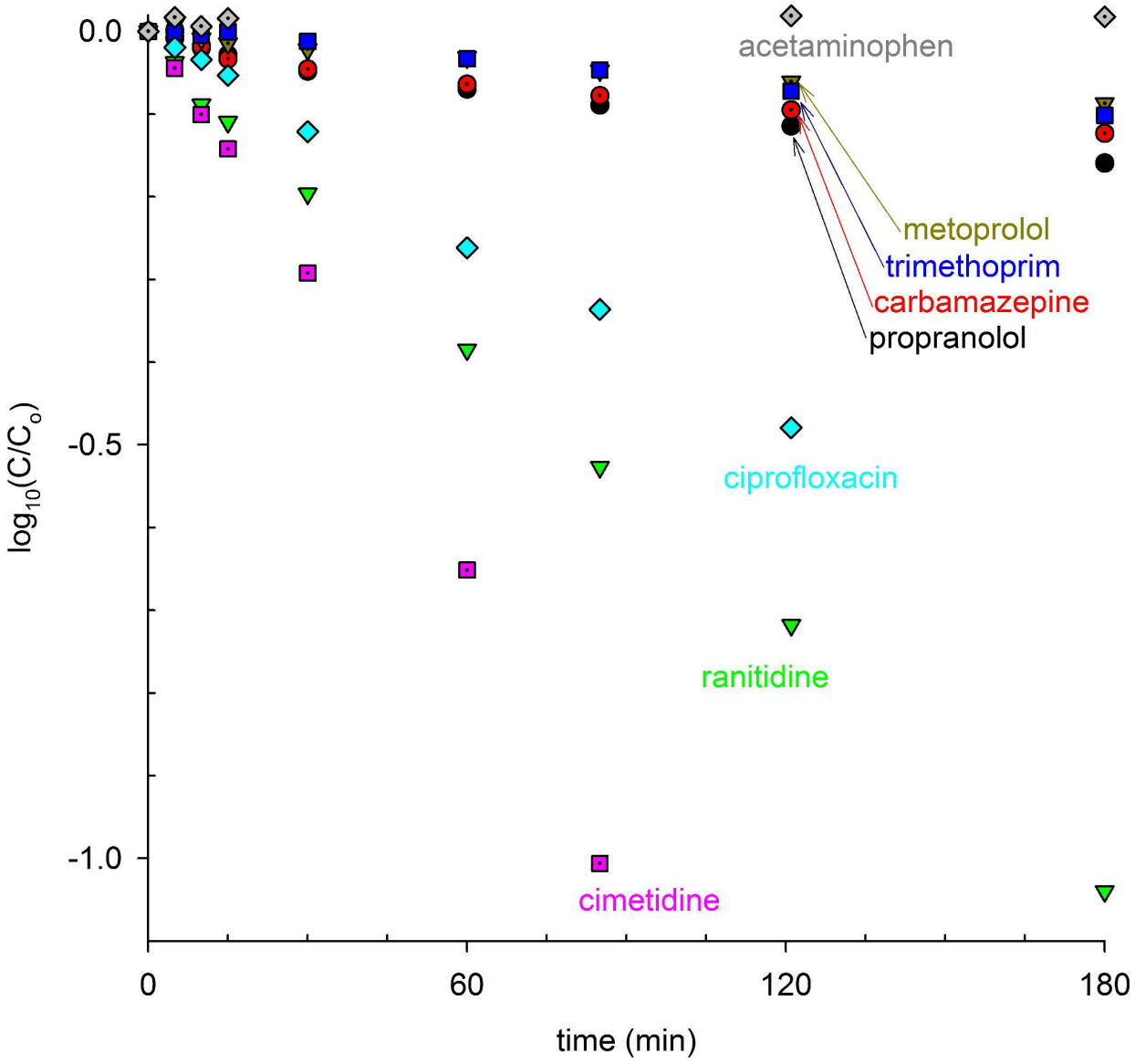

174

175 Figure SI 4. Test compound removal during electrolysis (3.5 V; 0.6 A L^{-1}) in water buffered at

176 pH 8.7 (20 mM borate).

177

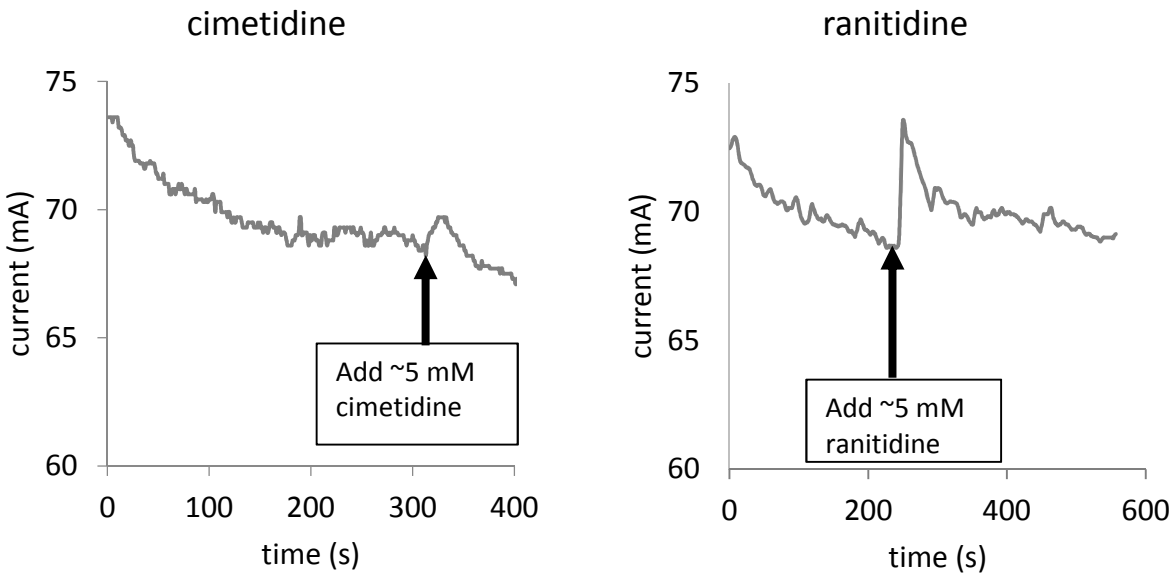

178

179 Figure SI 5. Current during addition of solid test compounds to solutions of Na_2SO_4 (20 mM)
180 undergoing electrolysis (3.5 V). Spikes in current upon test compound addition imply direct
181 electron transfer from the compound.

182

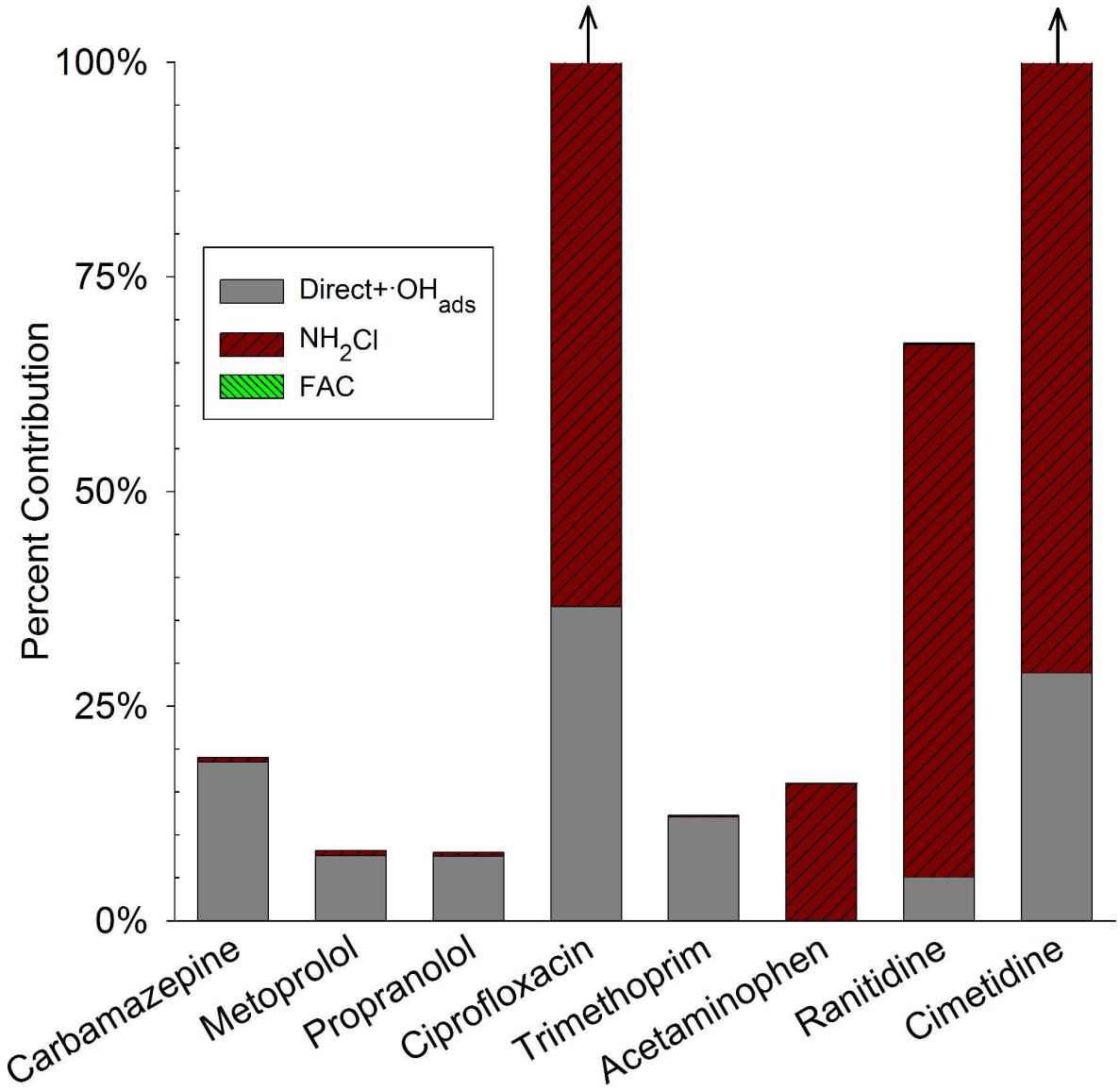

183

184 Figure SI 6. Calculated contributions of transformation mechanisms to test compound removal
185 in latrine wastewater electrolyzed at 3.5 V (0.7 A L^{-1}). Ciprofloxacin and cimetidine removal
186 rates were over-predicted by reaction with NH_2Cl.

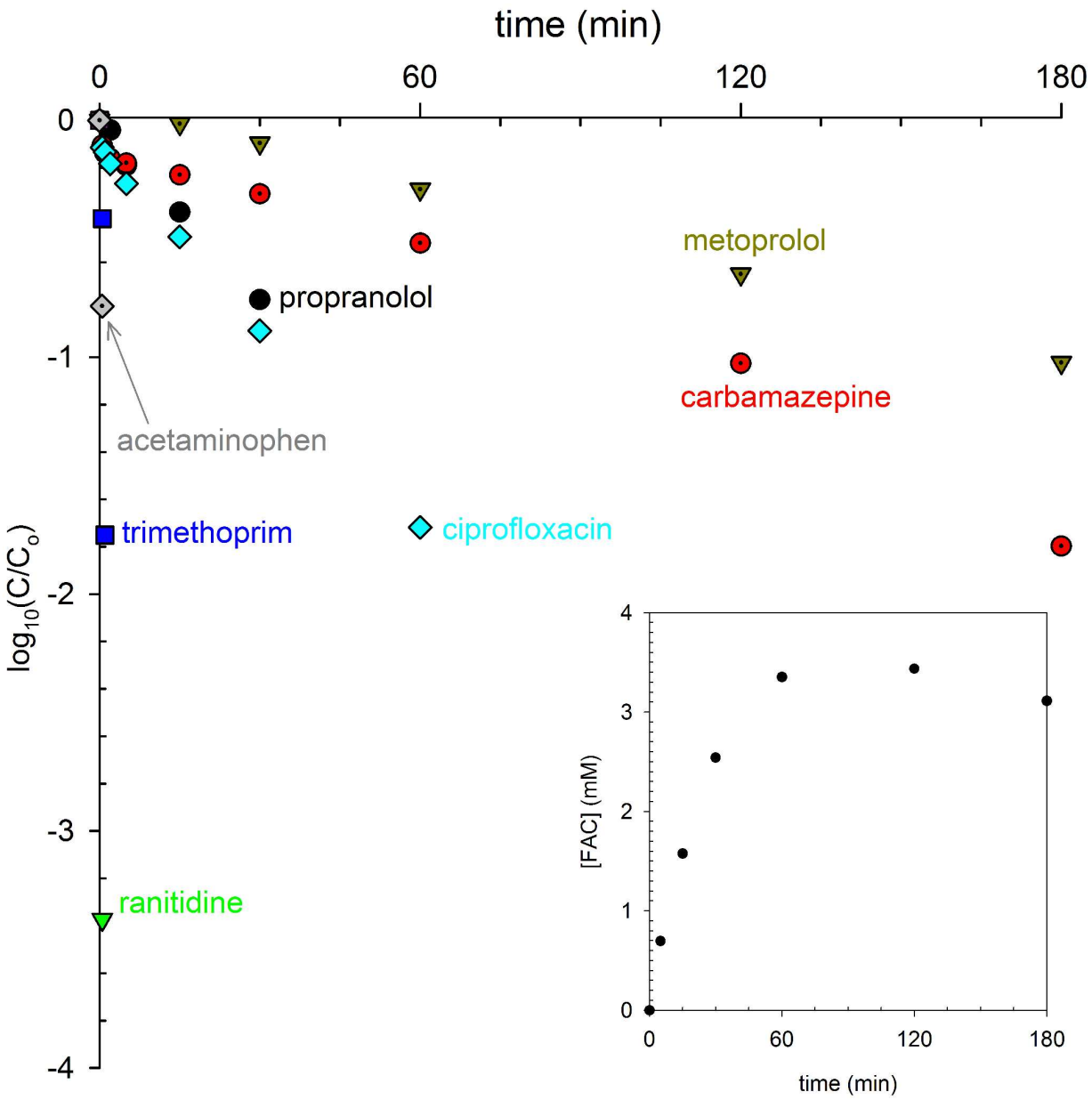

Figure SI 7. Test compound removal during electrolysis (3.5 V; 0.9 A L^{-1}) in 30 mM NaCl solution buffered at pH 8.7 (20 mM borate). Inset: [FAC] ([HOCl]+[OCl^-]) during electrolysis. Note that FAC concentrations plateaued after ~60 min due to FAC reduction on the cathode.[28]

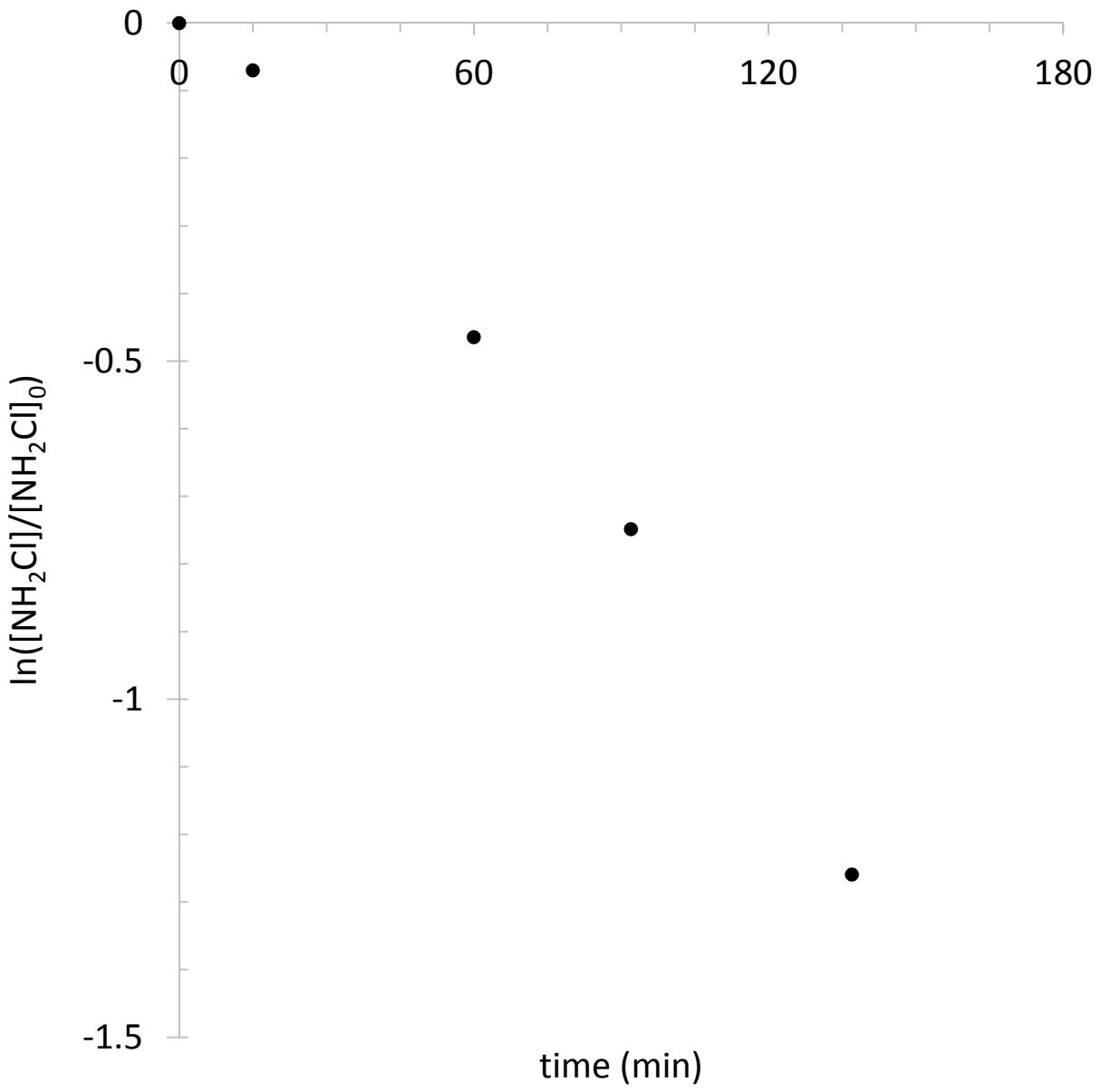

Figure SI 8. NH_2Cl reduction in buffered solution (pH 8.7) on a stainless steel cathode ($k=0.02\ C^{-1}$). The experiment was performed in an H cell with anodic and cathodic chambers separated by a Nafion membrane to prevent formation of chloramines at the anode. The cathodic potential was controlled at a similar potential to that observed during wastewater electrolysis (i.e., about -1.5 V vs. an Ag/AgCl/Sat. NaCl reference electrode; 10 mA). $[NH_2Cl]_0$=1 mM. Migration of NH_2Cl through the Nafion membrane was insignificant over the 2 hr experiment.

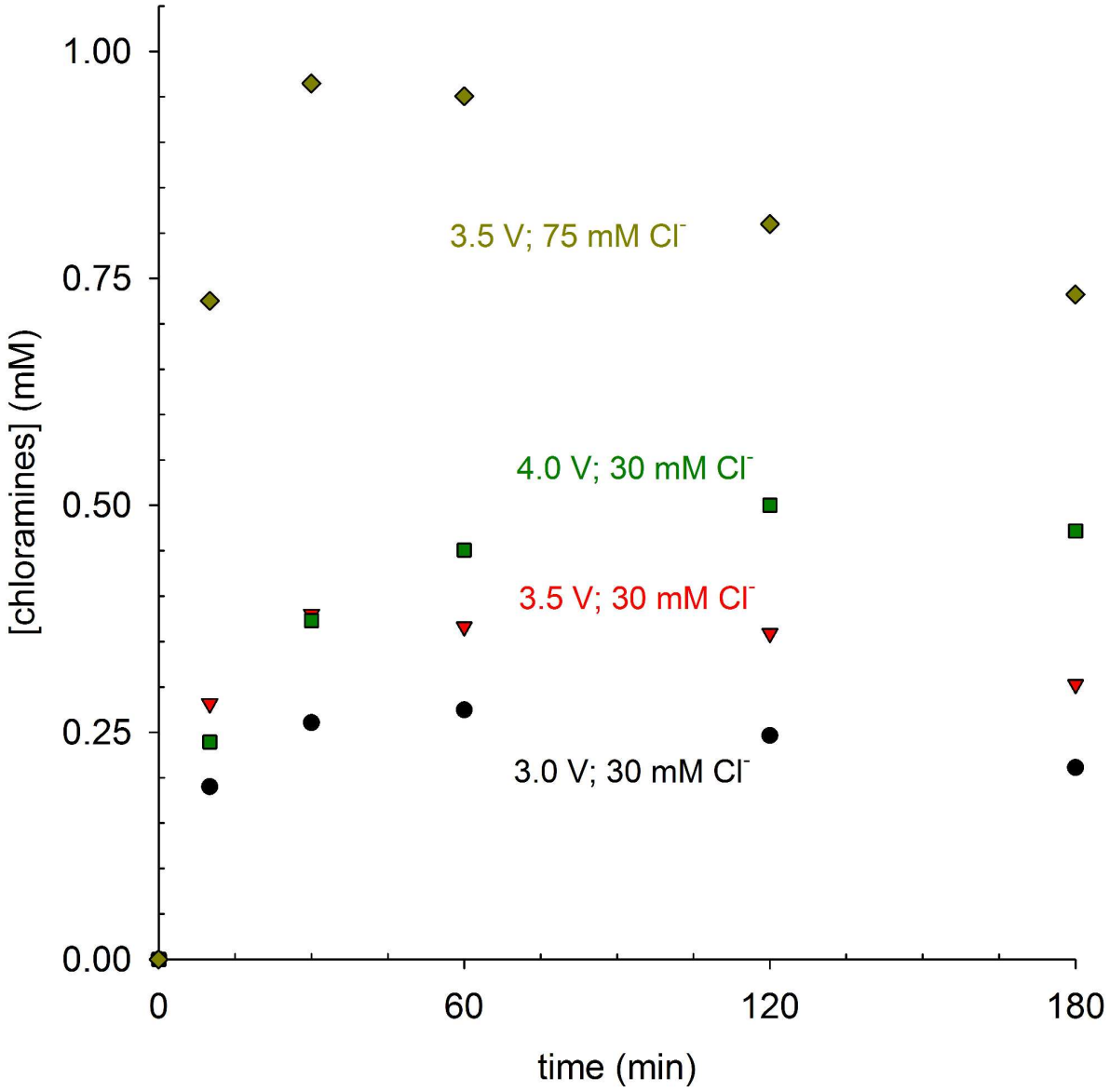

Figure SI 9. Chloramine concentration during electrolysis of latrine wastewater at various applied potentials (3.0-4.0 V) and chloride concentrations (30 mM; 75 mM). Average current densities: 3.0 V, 0.5 A L^{-1}; 3.5 V, 0.7 A L^{-1}; 4.0 V, 1.3 A L^{-1}; 3.5 V 75 mM Cl^-, 1.1 A L^{-1}.

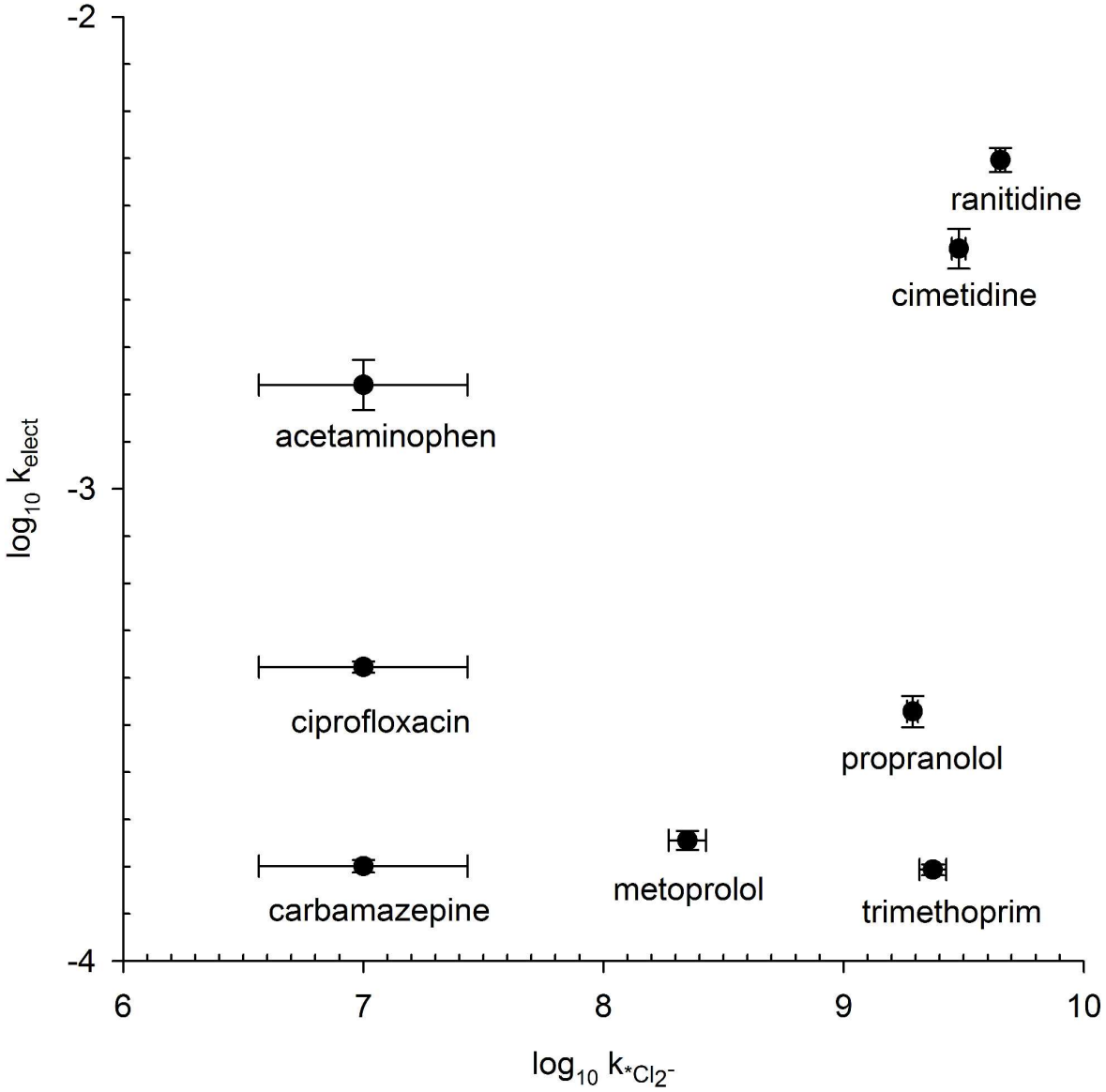

Figure SI 10. Correlation between test compound pseudo-first order electrolysis rates (k_{elect}; s^{-1}) in latrine wastewater at an applied potential of 3.5 V and measured second-order reaction rates with $\cdot Cl_2^-$ ($k_{\cdot Cl2-}$; M^{-1} s^{-1}). $\cdot Cl_2^-$ reaction rates with compounds that were too slow to measure by flash photolysis (carbamazepine, ciprofloxacin, and acetaminophen) were assumed to be between $10^{6.5}$ and $10^{7.5}$ M^{-1} s^{-1}. Error bars represent ± one standard deviation.

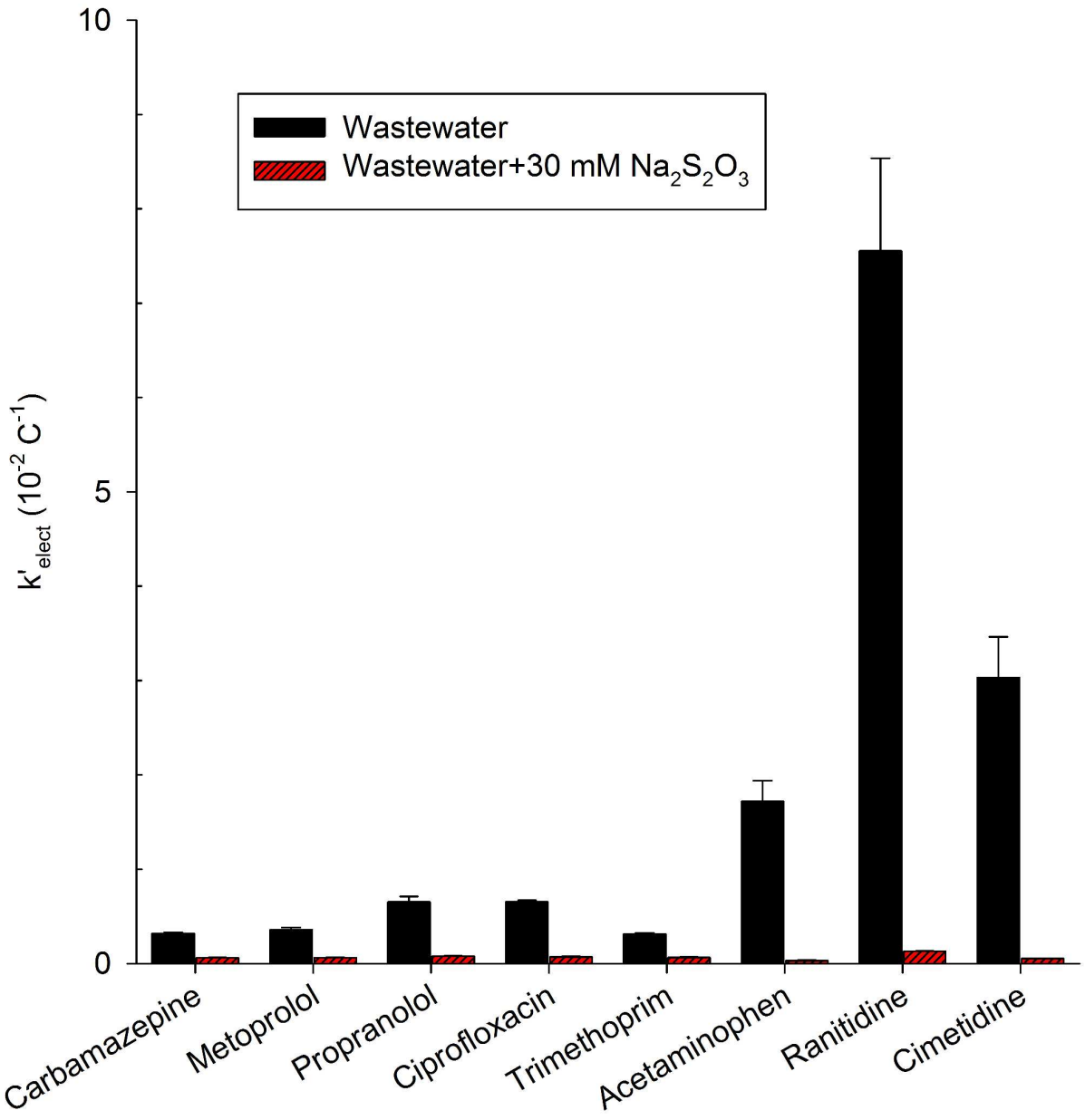

Figure SI 11. Pseudo-first order test compound electrolysis rates normalized for charge (k′) in latrine wastewater with or without added $Na_2S_2O_3$. Solutions were electrolyzed at an applied potential of 3.5 V. Average current densities: Wastewater, 0.7 A L^{-1}; Wastewater+30 mM $Na_2S_2O_3$, 0.9 A L^{-1}. Average chloramine concentration: Wastewater, 0.3 mM; Wastewater+30 mM $Na_2S_2O_3$, 0 mM. Error bars represent ± one standard deviation.

217 **a**

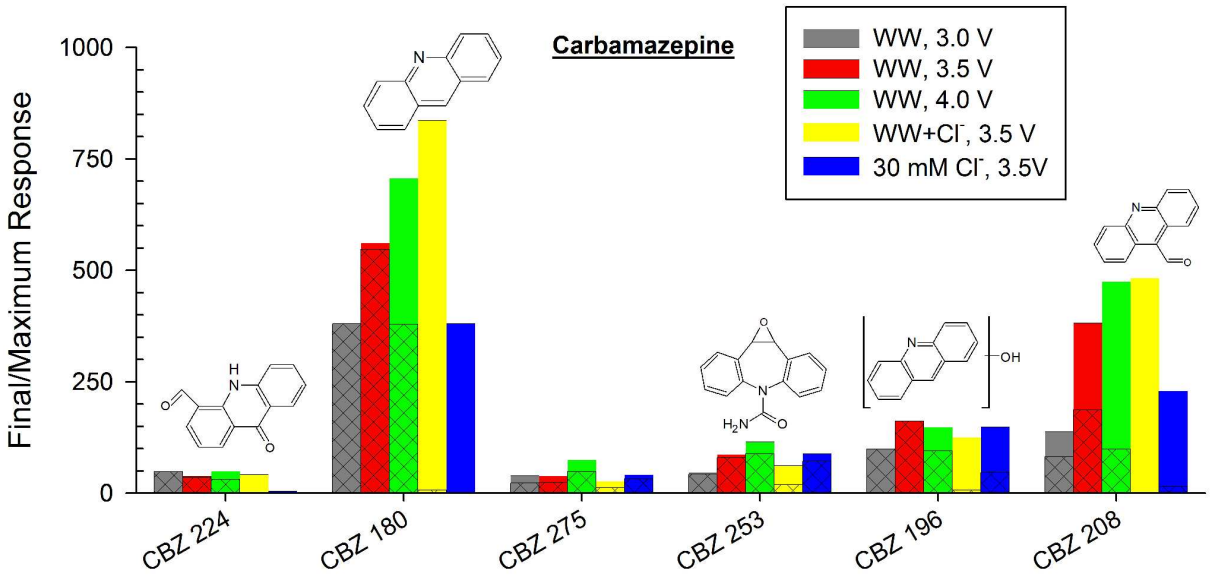

218

219 **b**

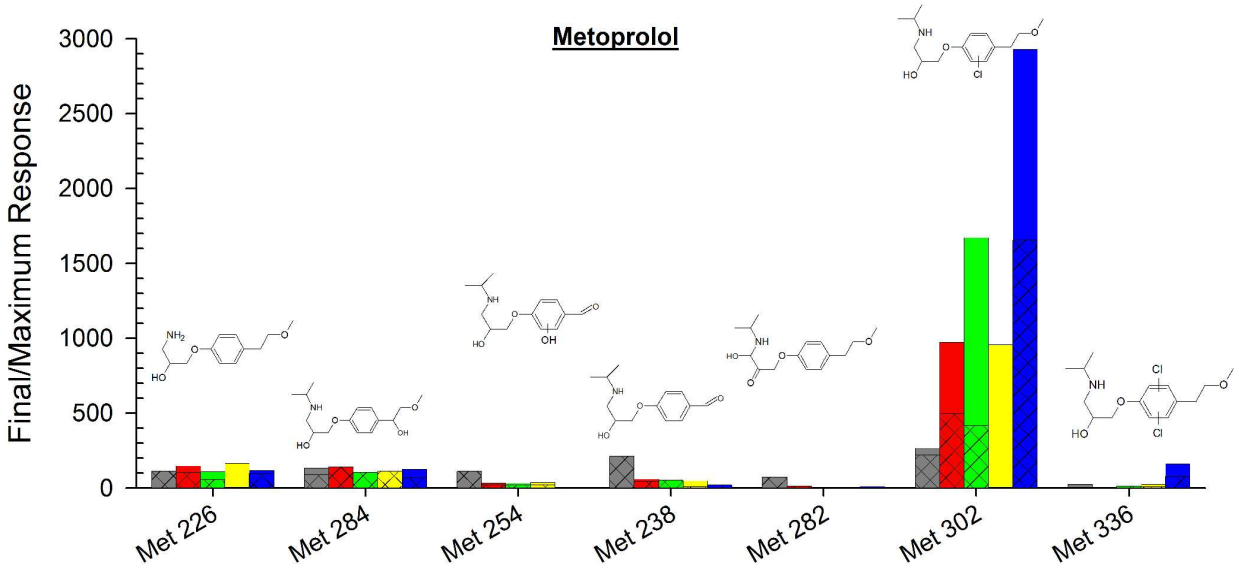

220

221 **c**

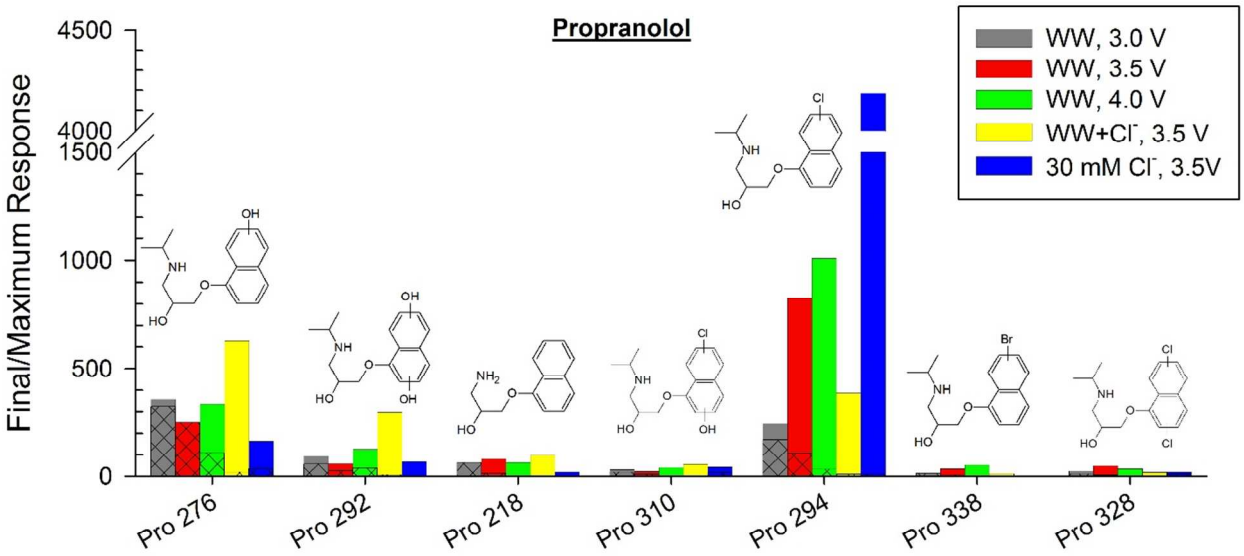

222

223 **d**

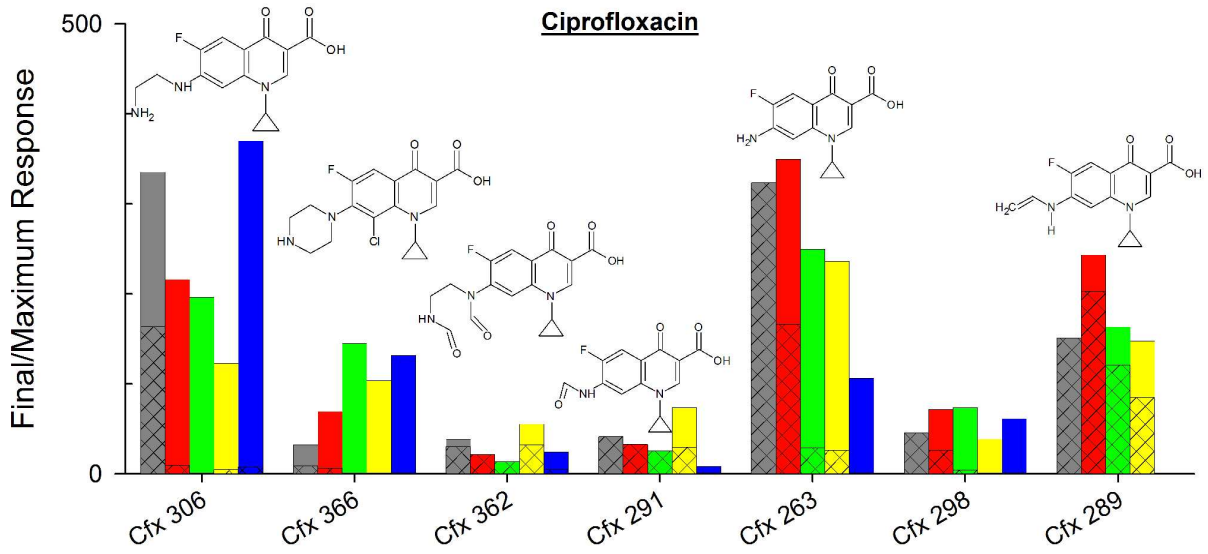

224

225 **e**

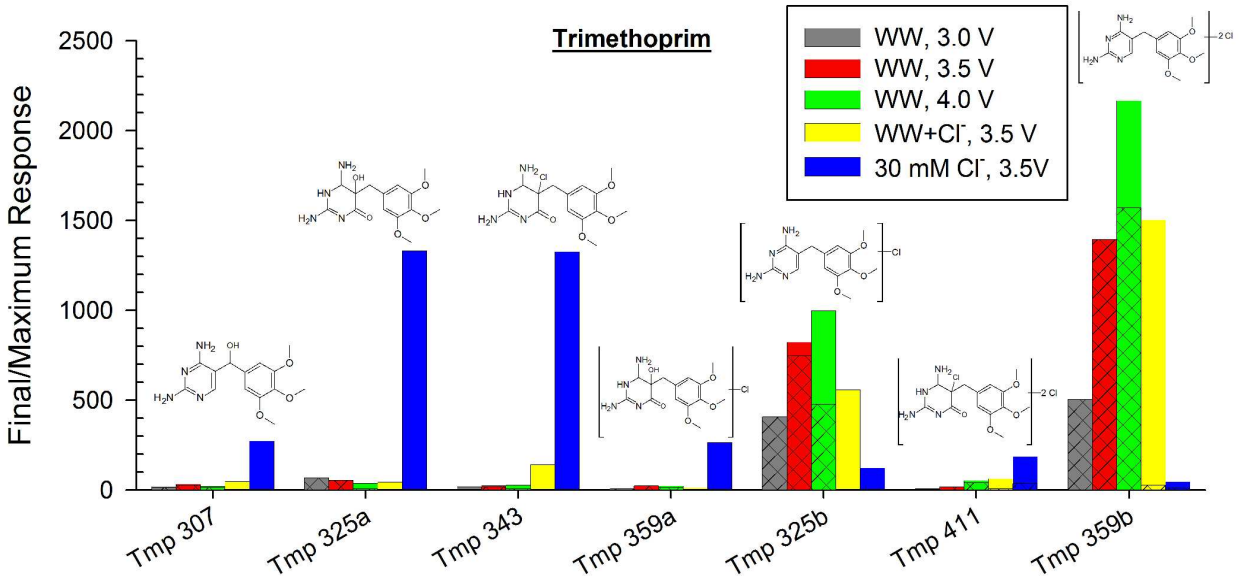

226

227 **f**

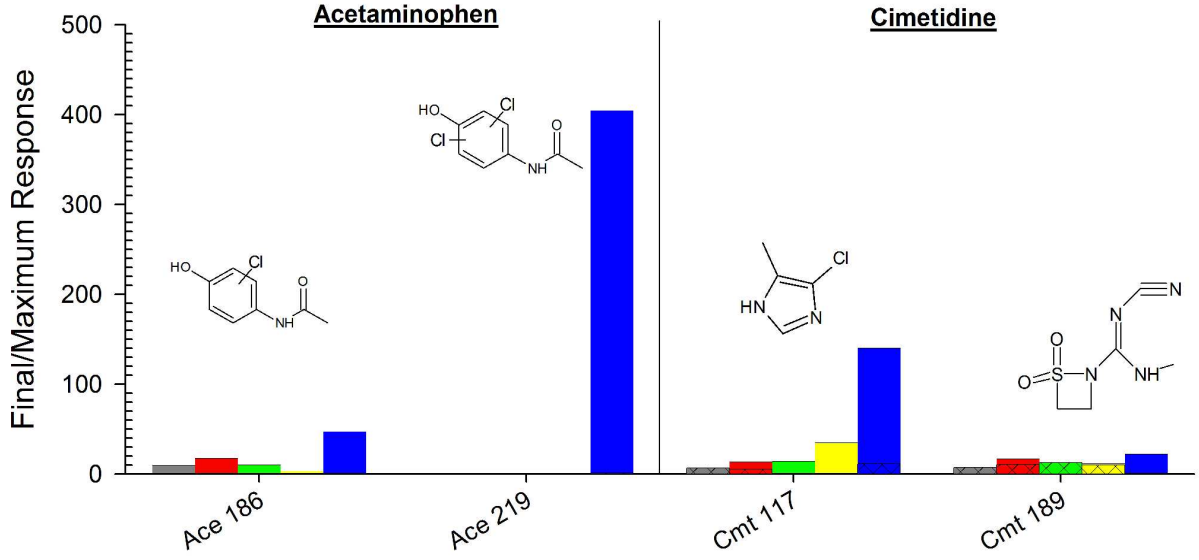

228

229 **g**

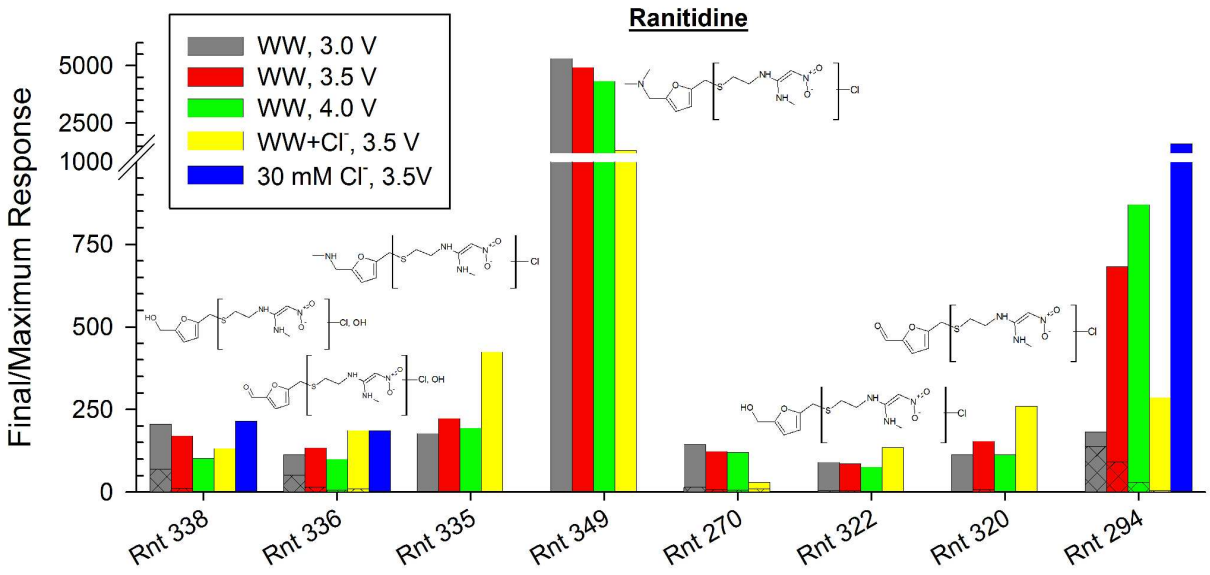

230

231 Figure SI 12. Maximum responses of predominant transformation product formed during
232 electrolysis (entire bar) and final amount remaining at end of electrolysis cycle (cross-hatched
233 portion). Electrolysis cycle was 180 min. Transformation product IDs represent the nominal
234 mass to charge ratio for each compound. Structures are proposed based on accurate mass to
235 charge ratios, fragments, and transformation products reported in the literature. Further
236 transformation product information is given in Table SI 2.

237

238 **a**

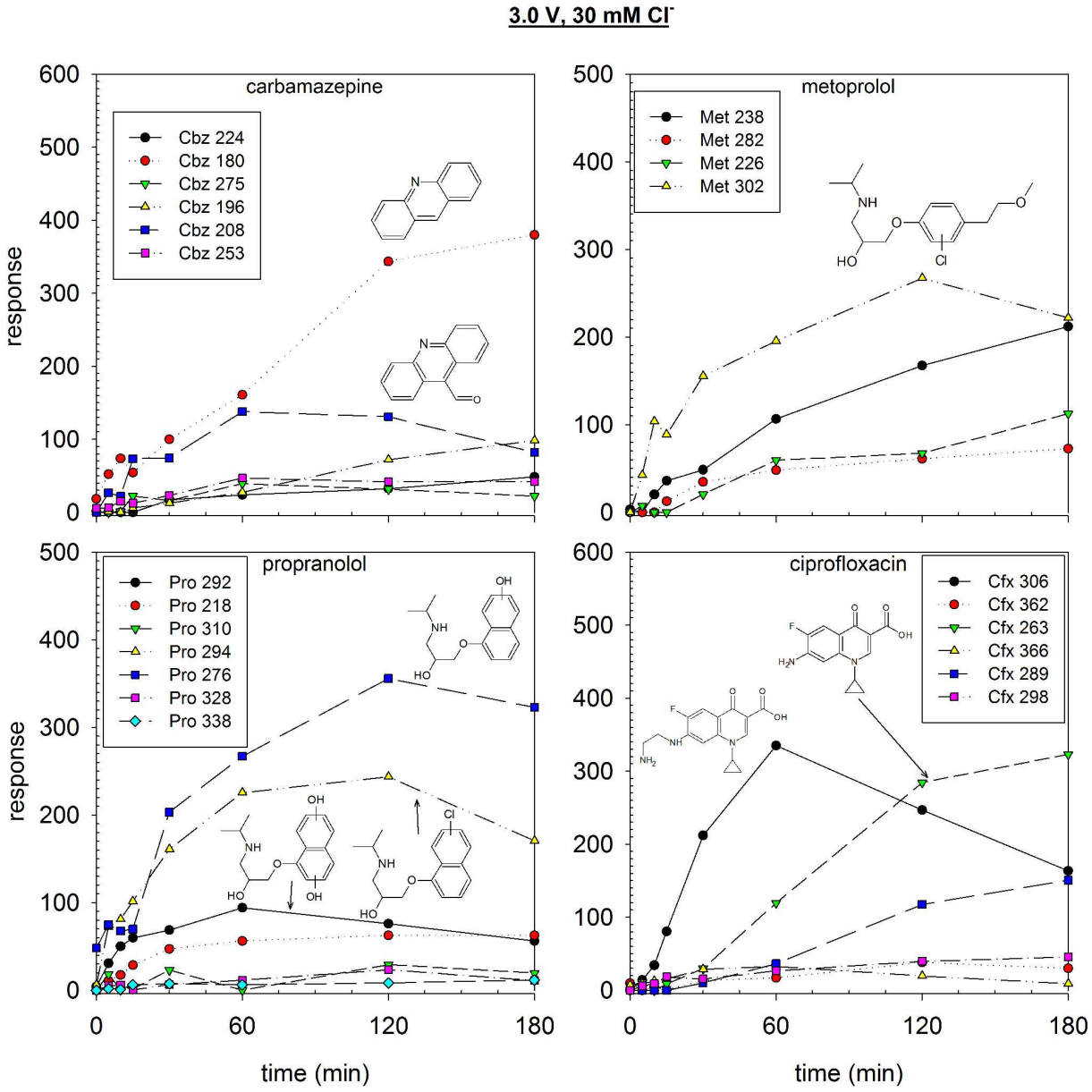

239

240

241

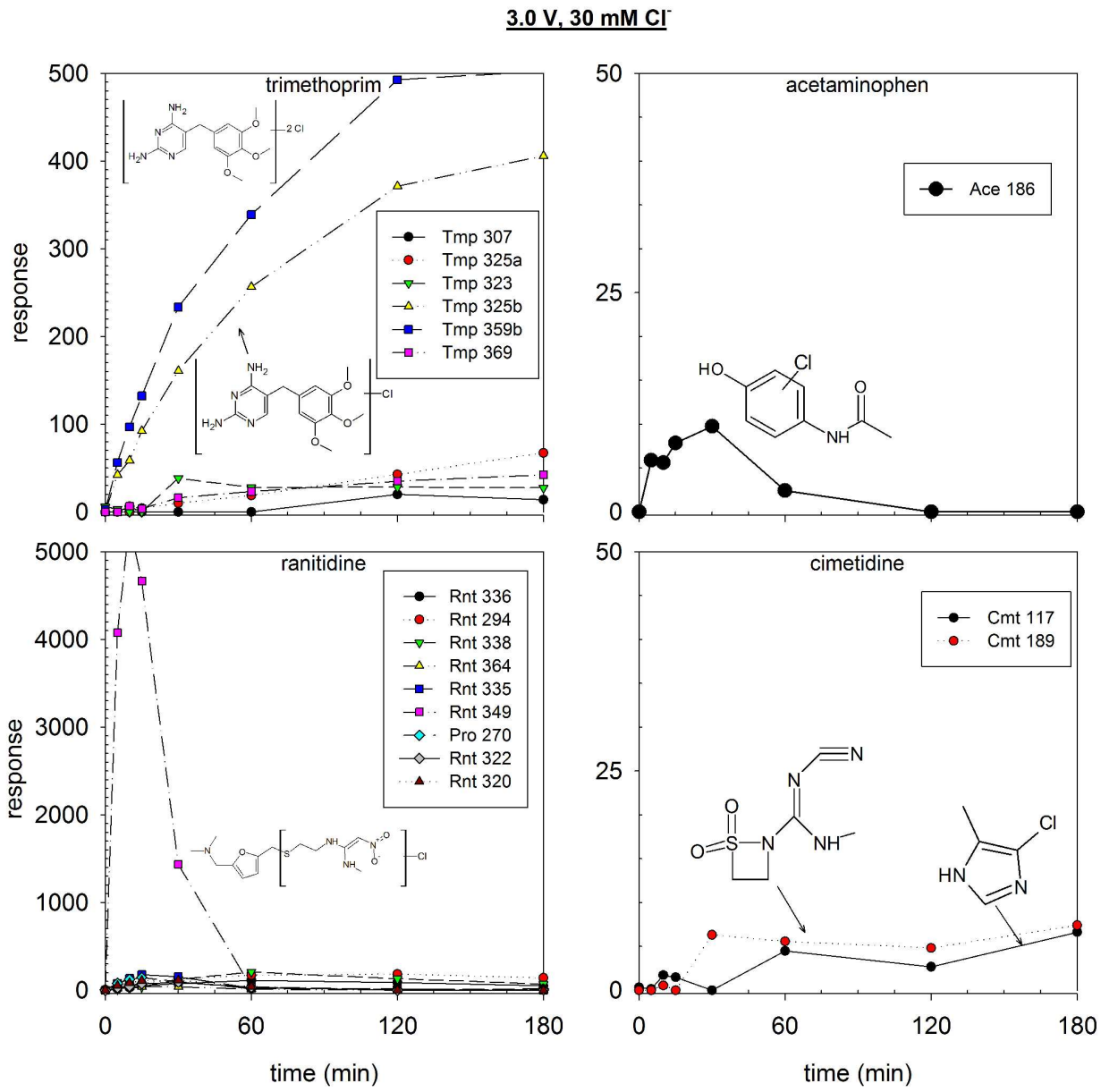

242

243 Figure SI 13a. Test compound transformation product formation during latrine wastewater
244 electrolysis at 3.0 V. Transformation product IDs represent the nominal mass to charge ratio for
245 each compound. Further transformation product information is given in Table SI 2.

246 **b**

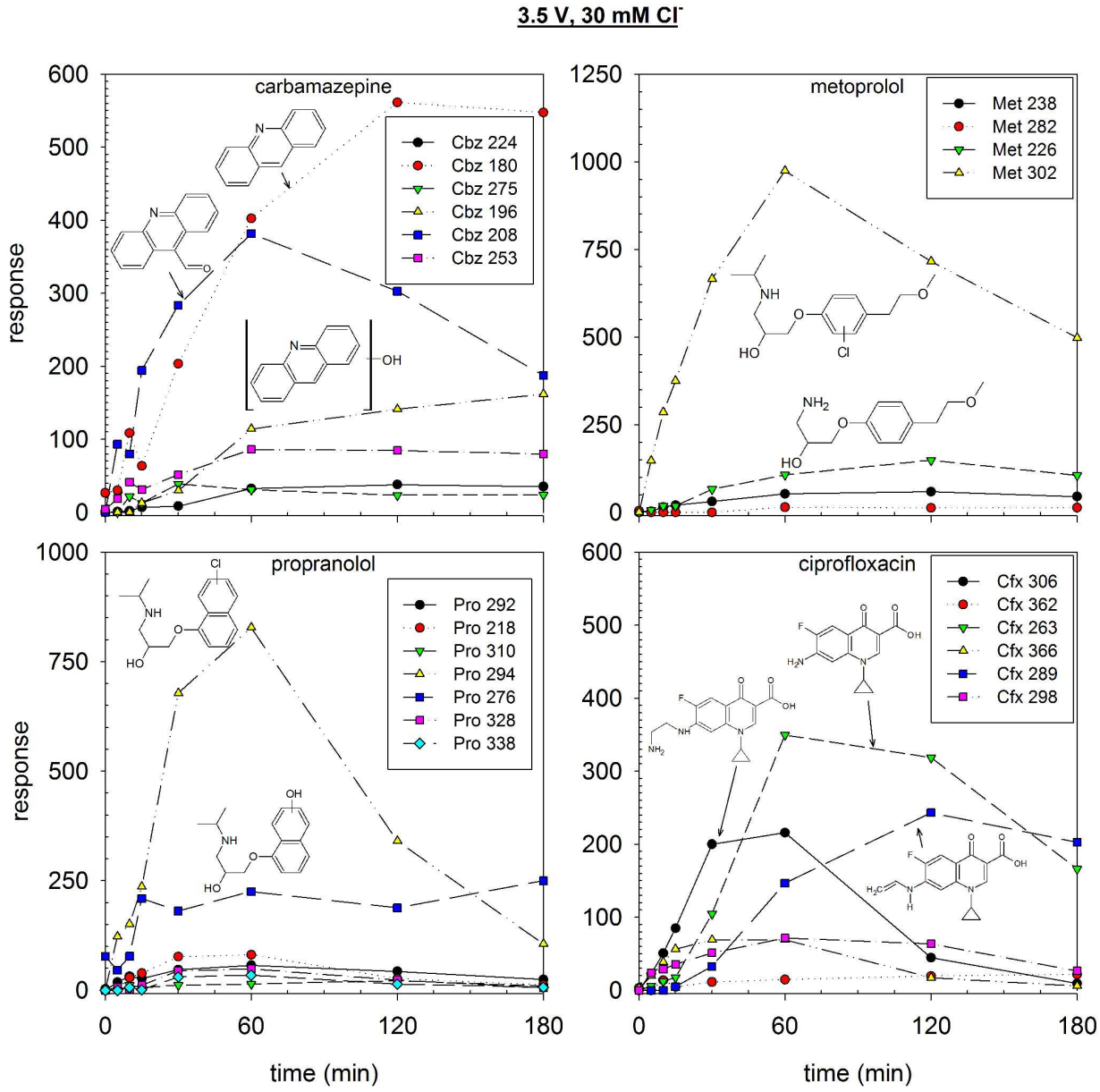
3.5 V, 30 mM Cl-
carbamazepine
Cbz 224
Cbz 180
Cbz 275
Cbz 196
Cbz 208
Cbz 253
metoprolol
Met 238
Met 282
Met 226
Met 302
propranolol
Pro 292
Pro 218
Pro 310
Pro 294
Pro 276
Pro 328
Pro 338
ciprofloxacin
Cfx 306
Cfx 362
Cfx 263
Cfx 366
Cfx 289
Cfx 298
response
time (min)

247

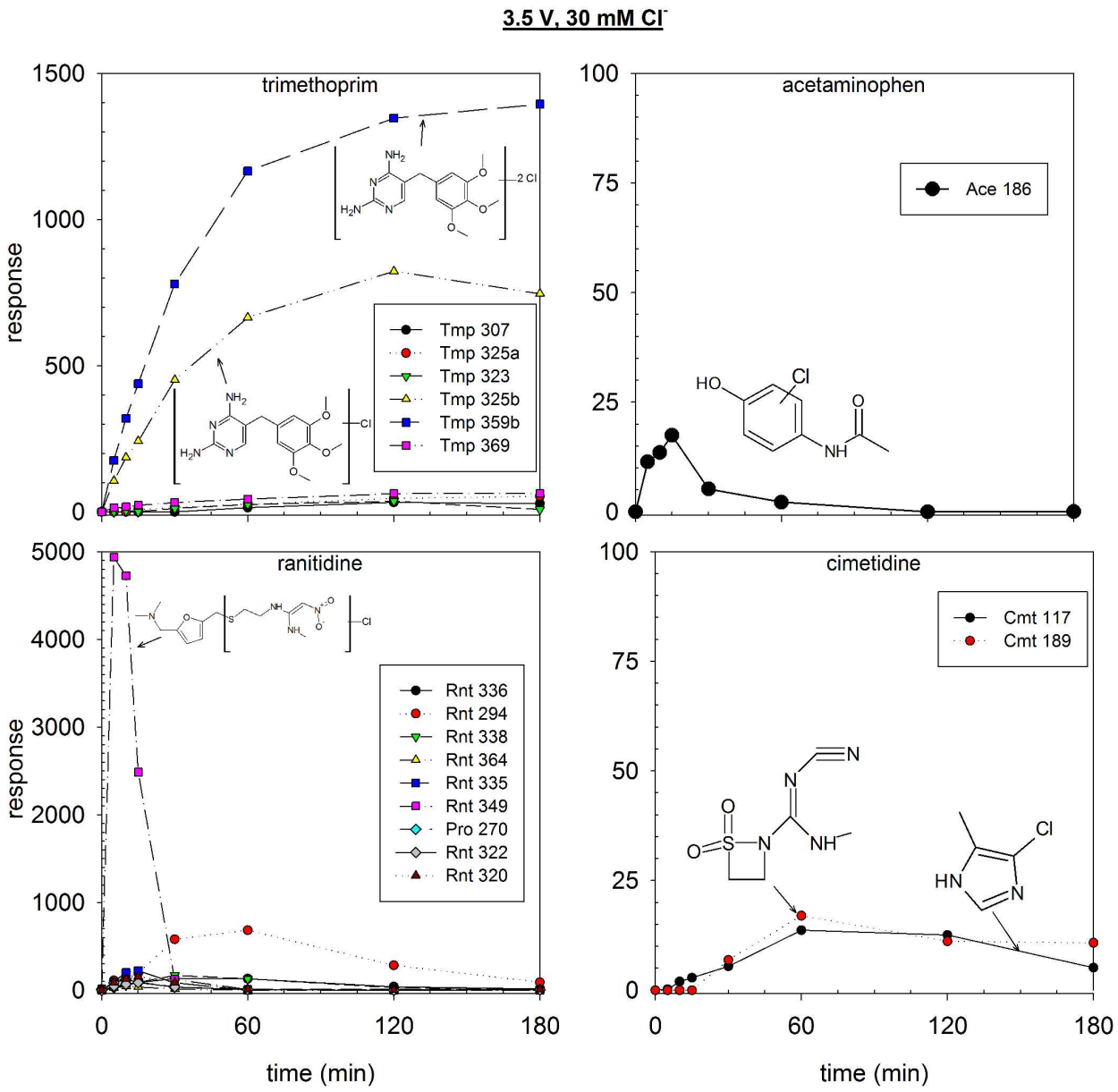

Figure SI 13b. Test compound transformation product formation during latrine wastewater electrolysis at 3.5 V. Transformation product IDs represent the nominal mass to charge ratio for each compound. Further transformation product information is given in Table SI 2.

252 **c**

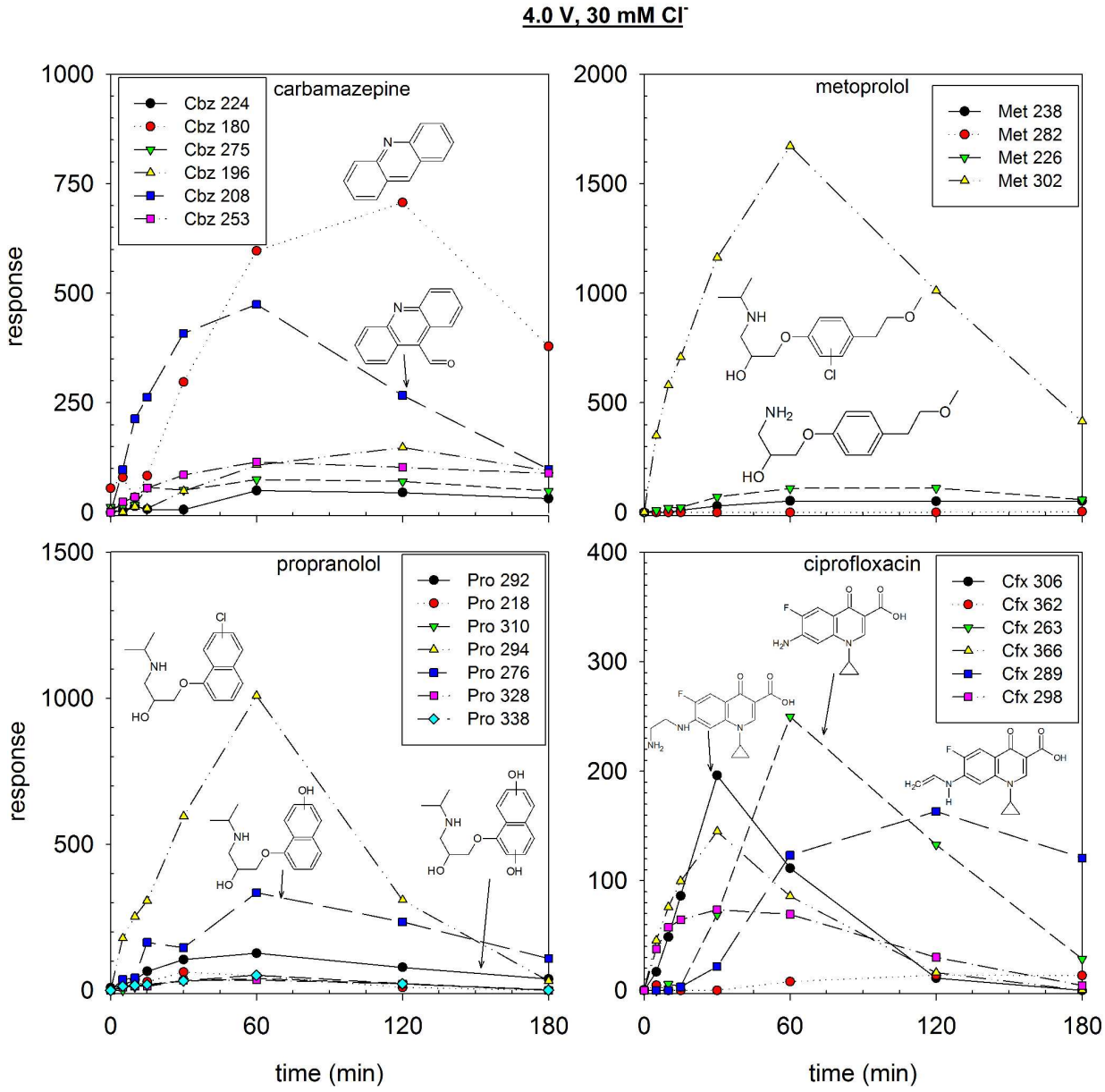
4.0 V, 30 mM Cl-
carbamazepine
Cbz 224
Cbz 180
Cbz 275
Cbz 196
Cbz 208
Cbz 253
metoprolol
Met 238
Met 282
Met 226
Met 302
propranolol
Pro 292
Pro 218
Pro 310
Pro 294
Pro 276
Pro 328
Pro 338
ciprofloxacin
Cfx 306
Cfx 362
Cfx 263
Cfx 366
Cfx 289
Cfx 298
response
time (min)

253

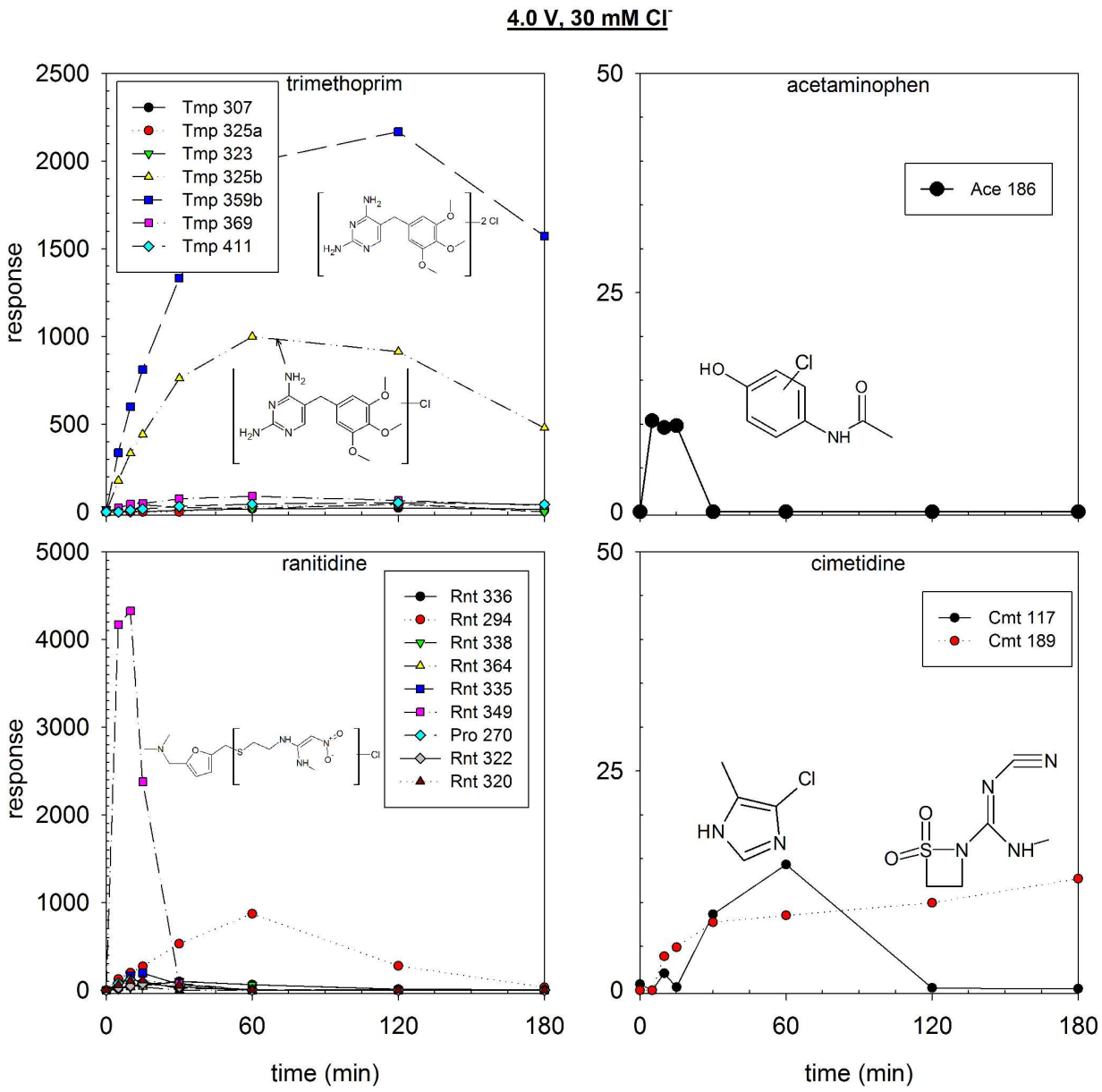

Figure SI 13c. Test compound transformation product formation during latrine wastewater electrolysis at 4.0 V. Transformation product IDs represent the nominal mass to charge ratio for each compound. Further transformation product information is given in Table SI 2.

258 **d**

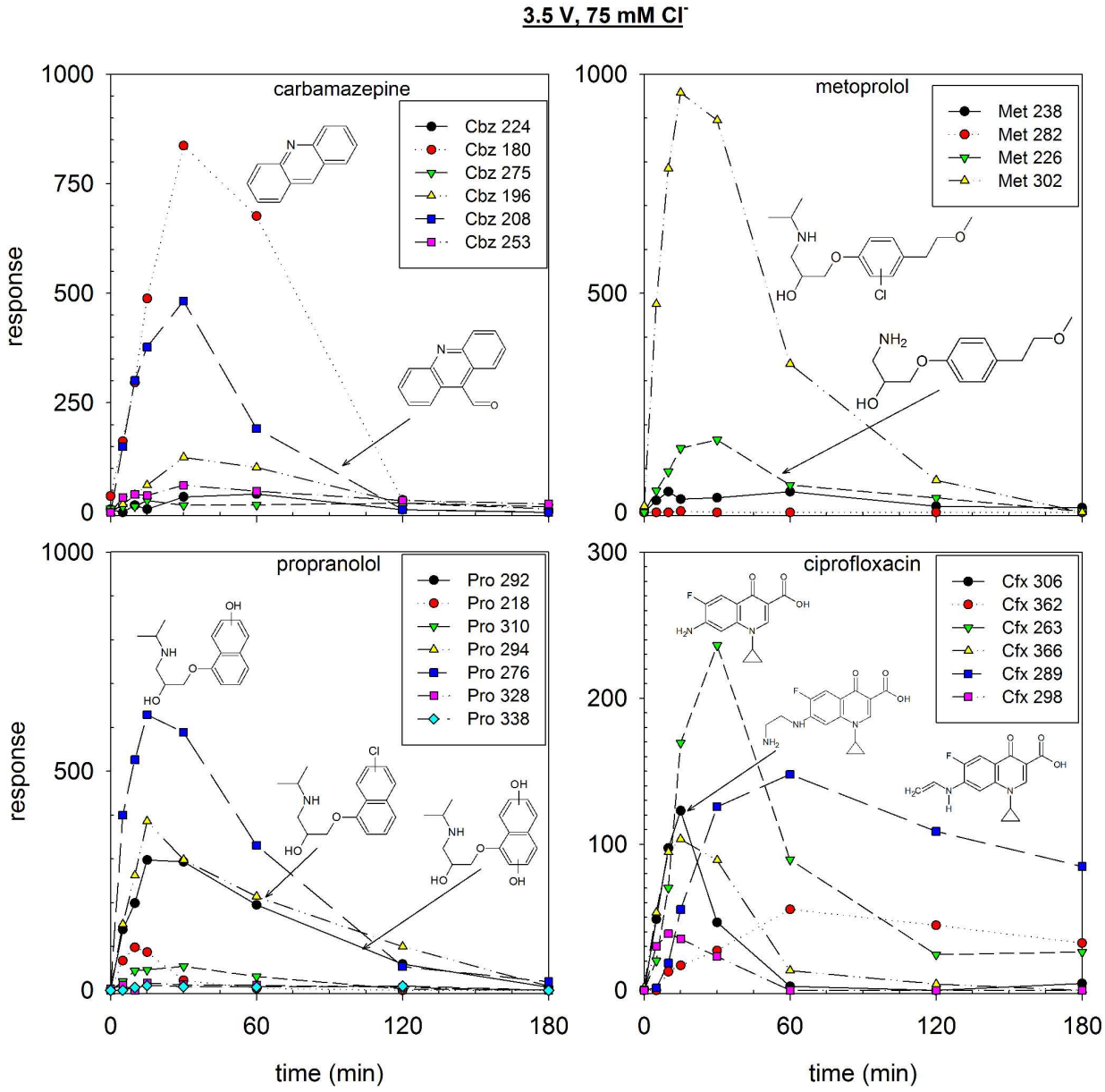
3.5 V, 75 mM Cl-
carbamazepine
Cbz 224
Cbz 180
Cbz 275
Cbz 196
Cbz 208
Cbz 253
metoprolol
Met 238
Met 282
Met 226
Met 302
propranolol
Pro 292
Pro 218
Pro 310
Pro 294
Pro 276
Pro 328
Pro 338
ciprofloxacin
Cfx 306
Cfx 362
Cfx 263
Cfx 366
Cfx 289
Cfx 298
response
time (min)

259

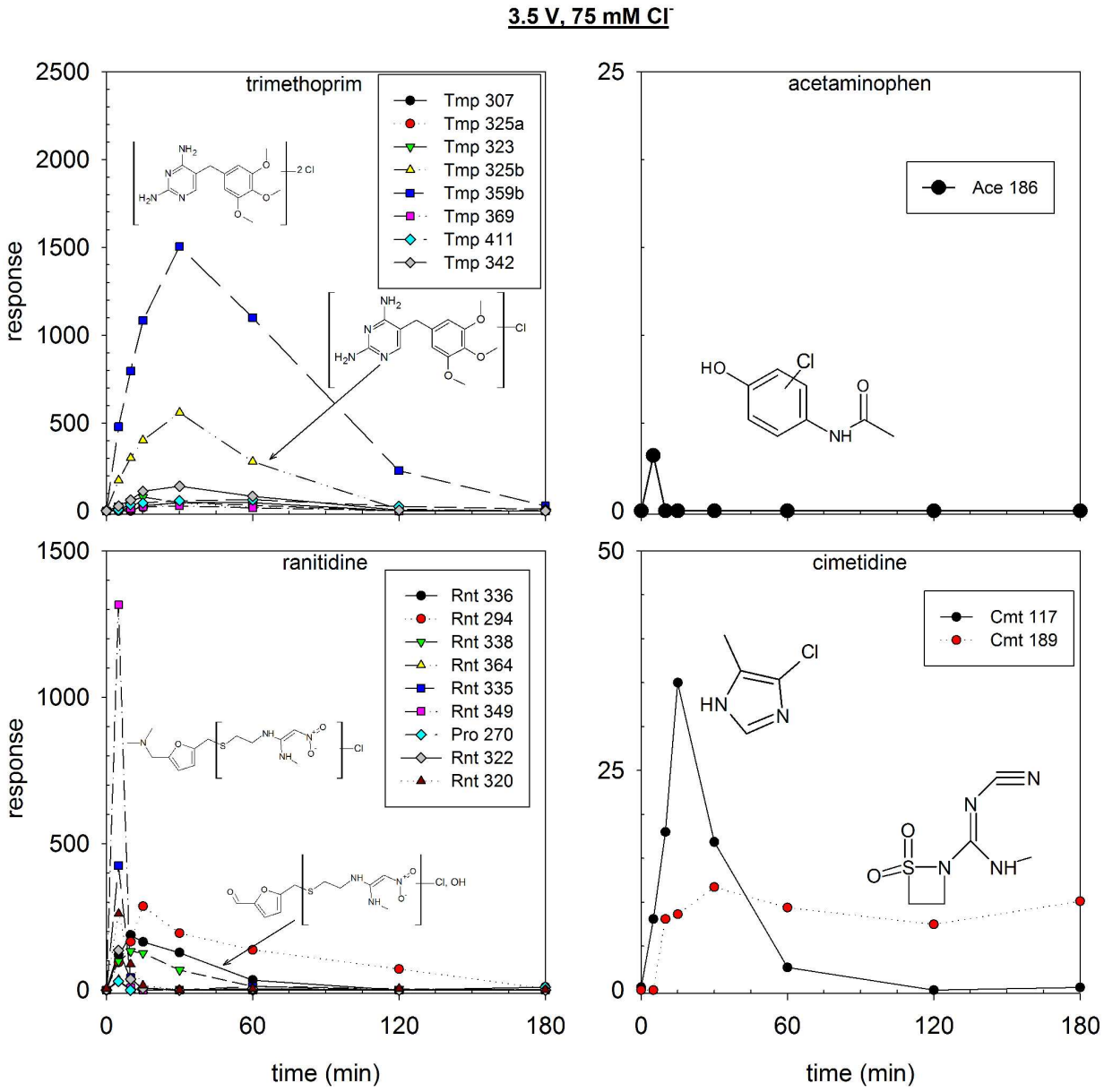

Figure SI 13d. Test compound transformation product formation during latrine wastewater electrolysis at 3.5 V with added NaCl. Transformation product IDs represent the nominal mass to charge ratio for each compound. Further transformation product information is given in Table SI 2.

265 **e**

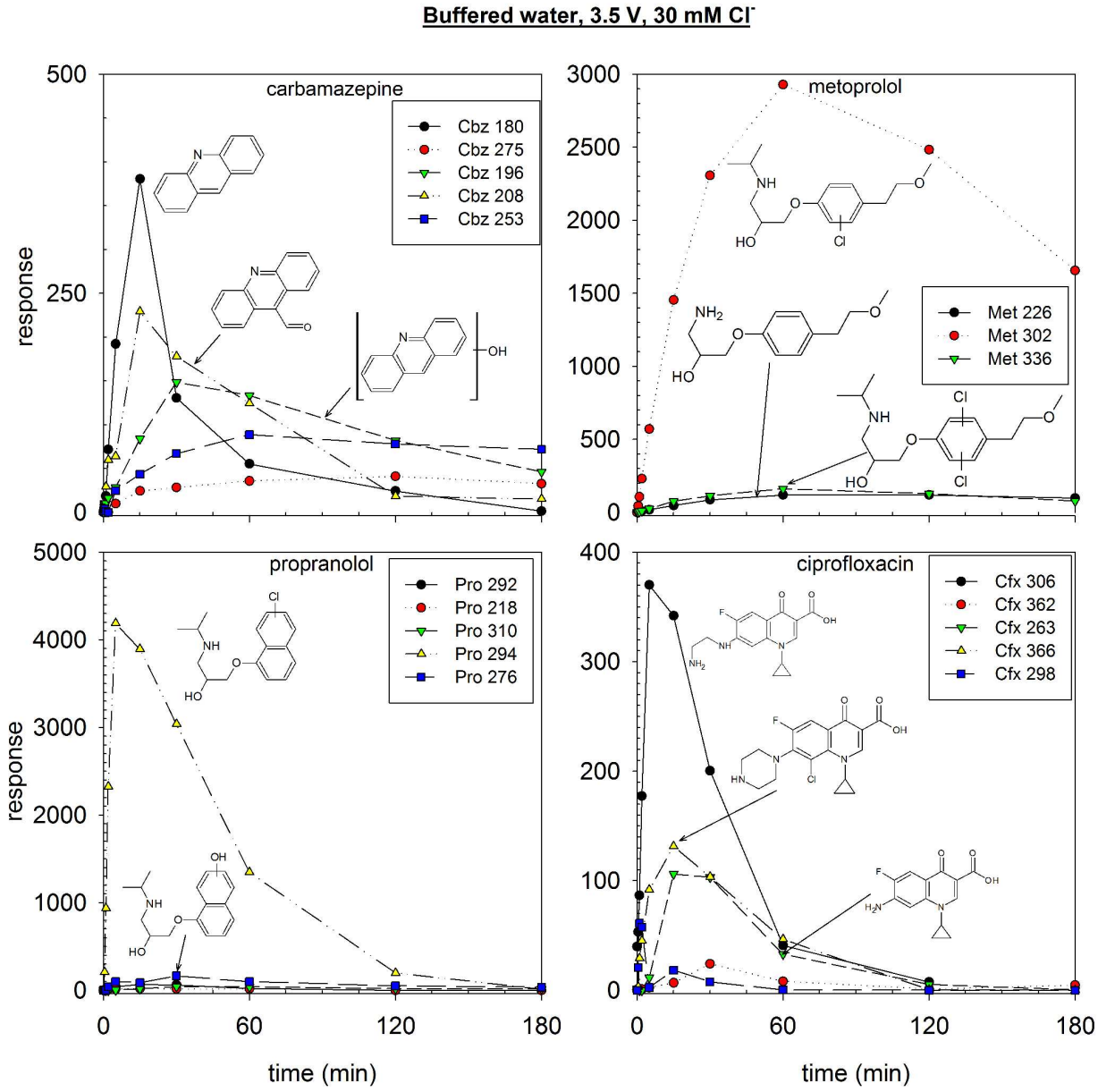
Buffered water, 3.5 V, 30 mM Cl-
carbamazepine
Cbz 180
Cbz 275
Cbz 196
Cbz 208
Cbz 253
metoprolol
Met 226
Met 302
Met 336
propranolol
Pro 292
Pro 218
Pro 310
Pro 294
Pro 276
ciprofloxacin
Cfx 306
Cfx 362
Cfx 263
Cfx 366
Cfx 298
response
time (min)

266

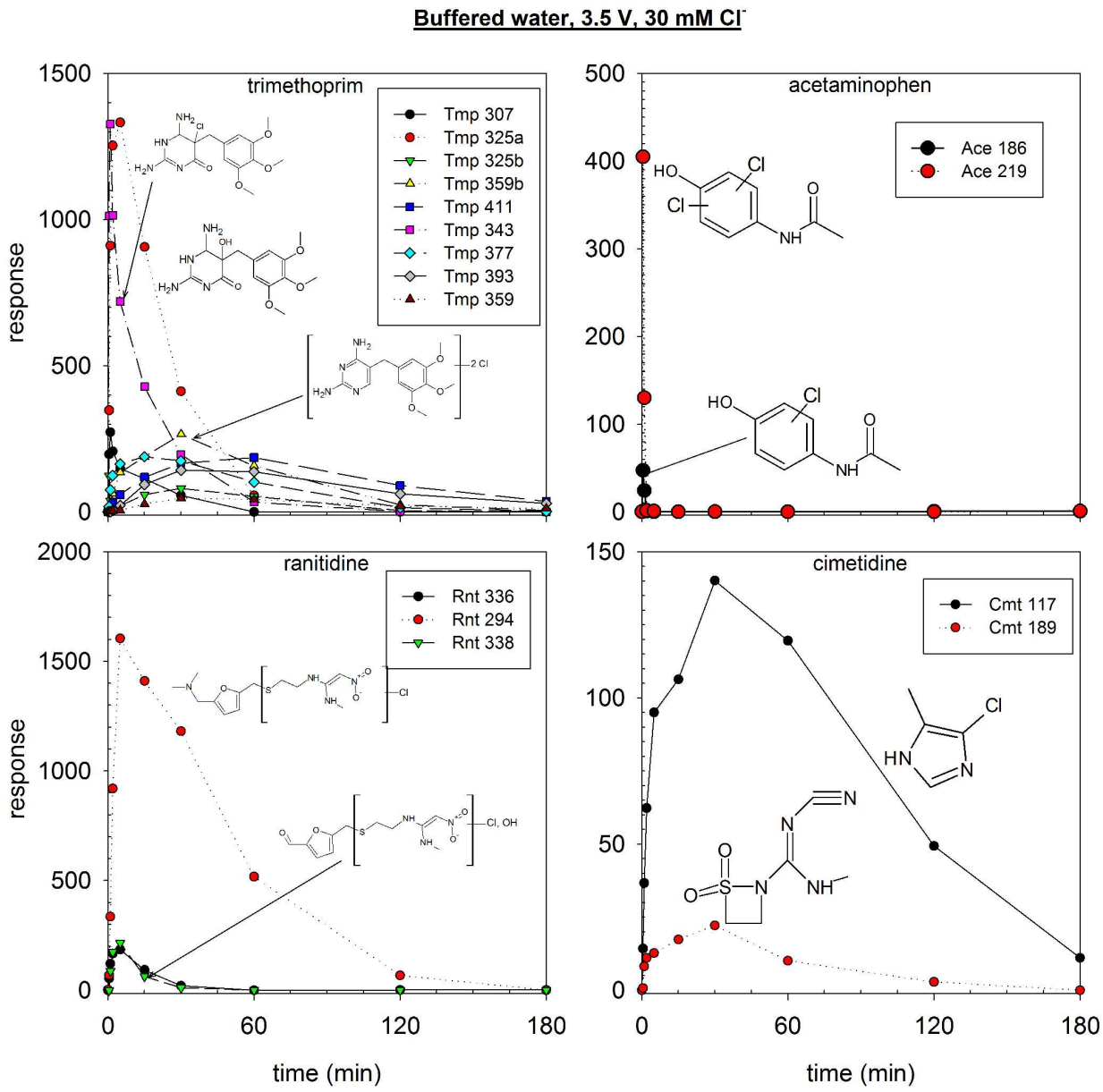

Figure SI 13e. Test compound transformation product formation during buffered Cl^- solution electrolysis. Transformation product IDs represent the nominal mass to charge ratio for each compound. Further transformation product information is given in Table SI 2.

References

(1) Alegre, M. L.; Geronés, M.; Rosso, J. A.; Bertolotti, S. G.; Braun, A. M.; Mártire, D. O.; Gonzalez, M. C. Kinetic Study of the Reactions of Chlorine Atoms and Cl2•- Radical Anions in Aqueous Solutions. 1. Reaction with Benzene. *J. Phys. Chem. A* **2000**, *104* (14), 3117–3125.

(2) Kesselman, J. M.; Weres, O.; Lewis, N. S.; Hoffmann, M. R. Electrochemical Production of Hydroxyl Radical at Polycrystalline Nb-Doped TiO2 Electrodes and Estimation of the Partitioning between Hydroxyl Radical and Direct Hole Oxidation Pathways. *J. Phys. Chem. B* **1997**, *101* (14), 2637–2643.

(3) Zhi, J.-F.; Wang, H.-B.; Nakashima, T.; Rao, T. N.; Fujishima, A. Electrochemical Incineration of Organic Pollutants on Boron-Doped Diamond Electrode. Evidence for Direct Electrochemical Oxidation Pathway. *J. Phys. Chem. B* **2003**, *107* (48), 13389–13395.

(4) American Public Health Association. *Standard Methods for the Examination of Water and Wastewater*, 19th ed.; American Public Health Association,, A. W. W. A., Water Environment Federation: Washington, DC, 1995.

(5) Wang, W.-L.; Wu, Q.-Y.; Huang, N.; Wang, T.; Hu, H.-Y. Synergistic effect between UV and chlorine (UV/chlorine) on the degradation of carbamazepine: Influence factors and radical species. *Water Res.* **2016**, *98*, 190–198.

(6) Hu, L.; Martin, H. M.; Arce-Bulted, O.; Sugihara, M. N.; Keating, K. A.; Strathmann, T. J. Oxidation of Carbamazepine by Mn(VII) and Fe(VI): Reaction Kinetics and Mechanism. *Environ. Sci. Technol.* **2009**, *43* (2), 509–515.

(7) Vogna, D.; Marotta, R.; Andreozzi, R.; Napolitano, A.; d'Ischia, M. Kinetic and chemical assessment of the UV/H2O2 treatment of antiepileptic drug carbamazepine. *Chemosphere* **2004**, *54* (4), 497–505.

(8) Geus, J. *Biotreatment of drinking water resources polluted by pesticides, pharmaceuticals and other micropollutants*; BIOTREAT; European Commission, 2014.

(9) Soufan, M.; Deborde, M.; Delmont, A.; Legube, B. Aqueous chlorination of carbamazepine: Kinetic study and transformation product identification. *Water Res.* **2013**, *47* (14), 5076–5087.

(10) Radjenovic, J.; Escher, B. I.; Rabaey, K. Electrochemical degradation of the β-blocker metoprolol by Ti/Ru0.7Ir0.3O2 and Ti/SnO2-Sb electrodes. *Water Res.* **2011**, *45* (10), 3205–3214.

(11) Veloutsou, S.; Bizani, E.; Fytianos, K. Photo-Fenton decomposition of β-blockers atenolol and metoprolol; study and optimization of system parameters and identification of intermediates. *Chemosphere* **2014**, *107*, 180–186.

(12) Svan, A.; Hedeland, M.; Arvidsson, T.; Jasper, J. T.; Sedlak, D. L.; Pettersson, C. E. Identification of transformation products from β-blocking agents formed in wetland microcosms using LC-Q-ToF. *J. Mass Spectrom.* **2016**, *51* (3), 207–218.

(13) Marcourrea, E.; Pereztrujillo, M.; Vicent, T.; Caminal, G. Ability of white-rot fungi to remove selected pharmaceuticals and identification of degradation products of ibuprofen by Trametes versicolor. *Chemosphere* **2009**, *74*, 765–772.

(14) Liu, Q.-T.; Williams, H. E. Kinetics and Degradation Products for Direct Photolysis of β-Blockers in Water. *Env. Sci Technol* **2007**, *41* (3), 803–810.

(15) Pinkston, K. E.; Sedlak, D. L. Transformation of Aromatic Ether- and Amine-Containing Pharmaceuticals during Chlorine Disinfection. *Environ. Sci. Technol.* **2004**, *38* (14), 4019–4025.
(16) Jasper, J. T.; Jones, Z. L.; Sharp, J. O.; Sedlak, D. L. Biotransformation of wastewater-derived trace organic contaminants in open-water unit process treatment wetlands. *Environ. Sci. Technol.* **2014**, *48* (9), 5136–5144.
(17) Dodd, M. C.; Shah, A. D.; von Gunten, U.; Huang, C.-H. Interactions of Fluoroquinolone Antibacterial Agents with Aqueous Chlorine: Reaction Kinetics, Mechanisms, and Transformation Pathways. *Environ. Sci. Technol.* **2005**, *39* (18), 7065–7076.
(18) Wang, P.; He, Y.-L.; Huang, C.-H. Oxidation of fluoroquinolone antibiotics and structurally related amines by chlorine dioxide: Reaction kinetics, product and pathway evaluation. *Water Res.* **2010**, *44* (20), 5989–5998.
(19) Anquandah, G. A. K.; Sharma, V. K.; Knight, D. A.; Batchu, S. R.; Gardinali, P. R. Oxidation of Trimethoprim by Ferrate(VI): Kinetics, Products, and Antibacterial Activity. *Environ. Sci. Technol.* **2011**, *45* (24), 10575–10581.
(20) Eichhorn, P.; Ferguson, P. L.; Pérez, S.; Aga, D. S. Application of Ion Trap-MS with H/D Exchange and QqTOF-MS in the Identification of Microbial Degradates of Trimethoprim in Nitrifying Activated Sludge. *Anal. Chem.* **2005**, *77* (13), 4176–4184.
(21) Dodd, M. C.; Huang, C.-H. Aqueous chlorination of the antibacterial agent trimethoprim: Reaction kinetics and pathways. *Water Res.* **2007**, *41* (3), 647–655.
(22) Bedner, M.; MacCrehan, W. A. Transformation of Acetaminophen by Chlorination Produces the Toxicants 1,4-Benzoquinone and N-Acetyl-p-benzoquinone Imine. *Environ. Sci. Technol.* **2006**, *40* (2), 516–522.
(23) Cao, F.; Zhang, M.; Yuan, S.; Feng, J.; Wang, Q.; Wang, W.; Hu, Z. Transformation of acetaminophen during water chlorination treatment: kinetics and transformation products identification. *Environ. Sci. Pollut. Res.* **2016**, *23* (12), 1–9.
(24) Buth, J. M.; Arnold, W. A.; McNeill, K. Unexpected Products and Reaction Mechanisms of the Aqueous Chlorination of Cimetidine. *Environ. Sci. Technol.* **2007**, *41* (17), 6228–6233.
(25) Le Roux, J.; Gallard, H.; Croué, J.-P.; Papot, S.; Deborde, M. NDMA Formation by Chloramination of Ranitidine: Kinetics and Mechanism. *Environ. Sci. Technol.* **2012**, *46* (20), 11095–11103.
(26) Acero, J. L.; Benitez, F. J.; Real, F. J.; Roldan, G. Kinetics of aqueous chlorination of some pharmaceuticals and their elimination from water matrices. *Water Res.* **2010**, *44* (14), 4158–4170.
(27) Gallard, H.; von Gunten, U. Chlorination of Phenols: Kinetics and Formation of Chloroform. *Environ. Sci. Technol.* **2002**, *36* (5), 884–890.
(28) Park, H.; Vecitis, C. D.; Hoffmann, M. R. Electrochemical Water Splitting Coupled with Organic Compound Oxidation: The Role of Active Chlorine Species. *J. Phys. Chem. C* **2009**, *113* (18), 7935–7945.